3.4 High speed trains with magnetic levitation

3.4.1 Active magnetically levitated high-speed train TRANSRAPID

3.4.2 Japanese electro-dynamically levitated high-speed train YAMANASHI

Yamanashi – MAGLEV railway

Source:
RTRI, Japan

Yamanashi: Arrangement of levitation and guidance coils at the sides

- **Levitation & guidance coils shaped in 8-form!**

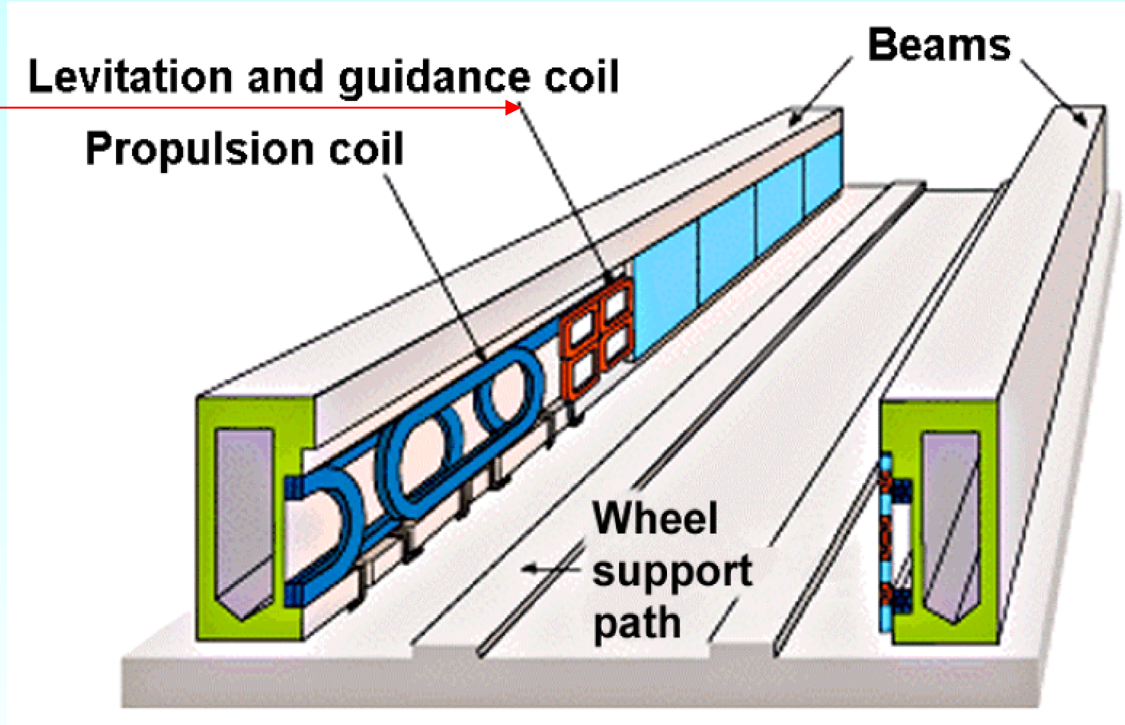

Source: RTRI, Japan

- **Aluminum short circuited magnet coils as levitation and guidance coils along the track sides**

- **Thus the track below the vehicle remains free for the rolling of the wheels before reaching the "Take-off"-velocity!**

Yamanashi: Voltage induction in the 8-coils

Flux linkage zero, current $I_p = 0$

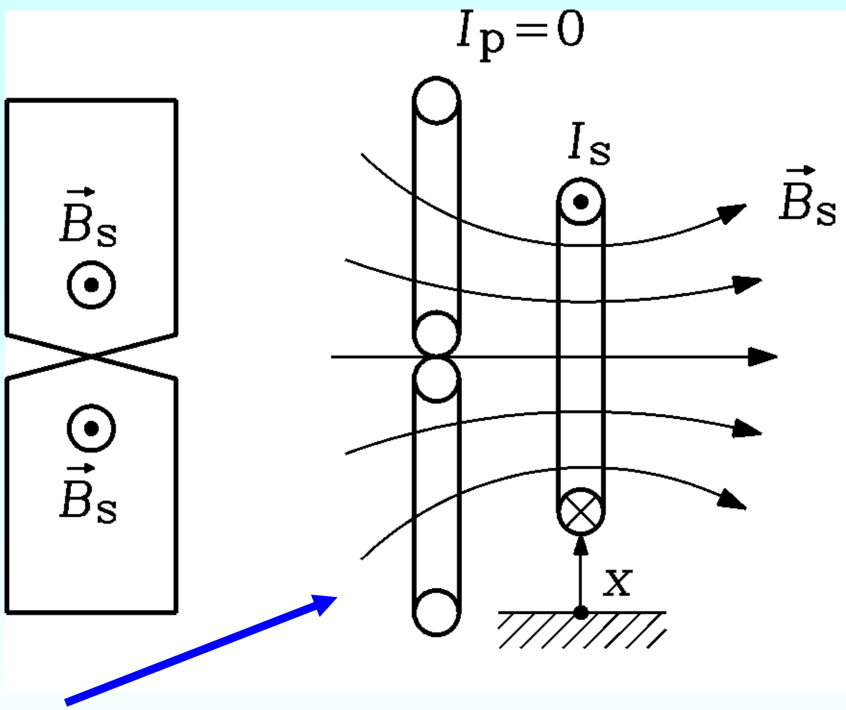

Flux linkage non-zero: $d\Phi_p/dt$ causes current I_p to flow!

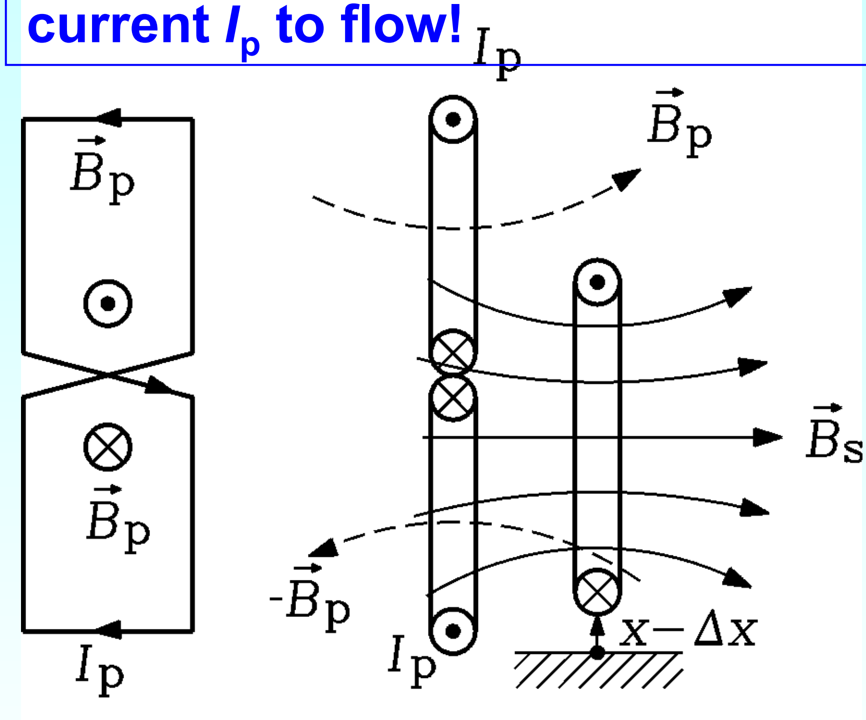

- Vertical "zero-flux"-condition: The DC excited superconducting coils on board of the moving vehicle excite via the current DC-current I_s a field B_s, which is linked with the 8-coils of the track sides.
- At the levitation distance *x* the total flux linkage in the 8-coils is **zero** due to symmetry: ⇒ No voltage induction occurs ⇒ no current flow I_p ⇒ no levitation force

Yamanashi: Generation of levitation force

Flux linkage non-zero: $d\Phi_p/dt$ causes current I_p to flow!

Current $I_p \rightarrow$ Levitation force F_{res}

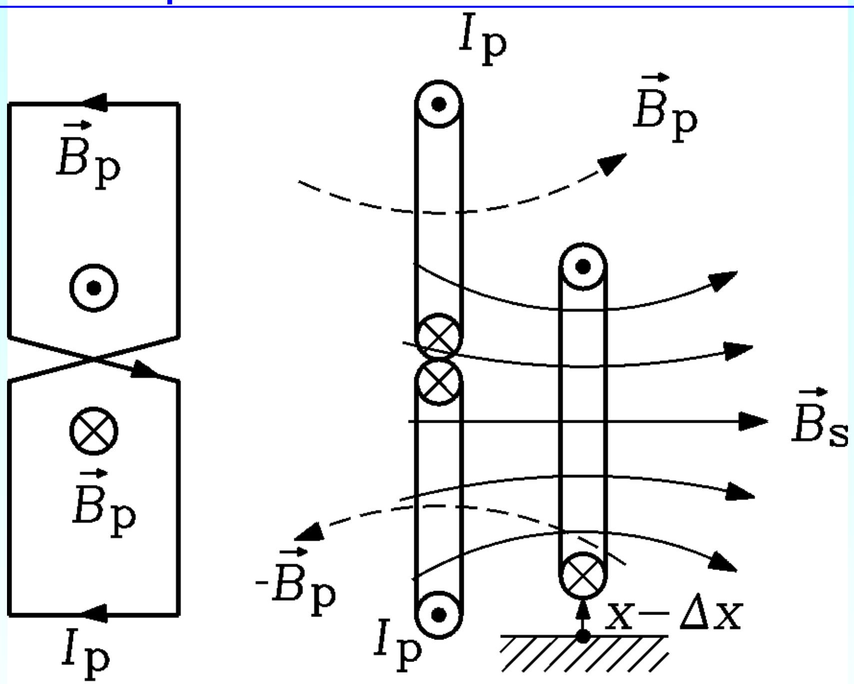

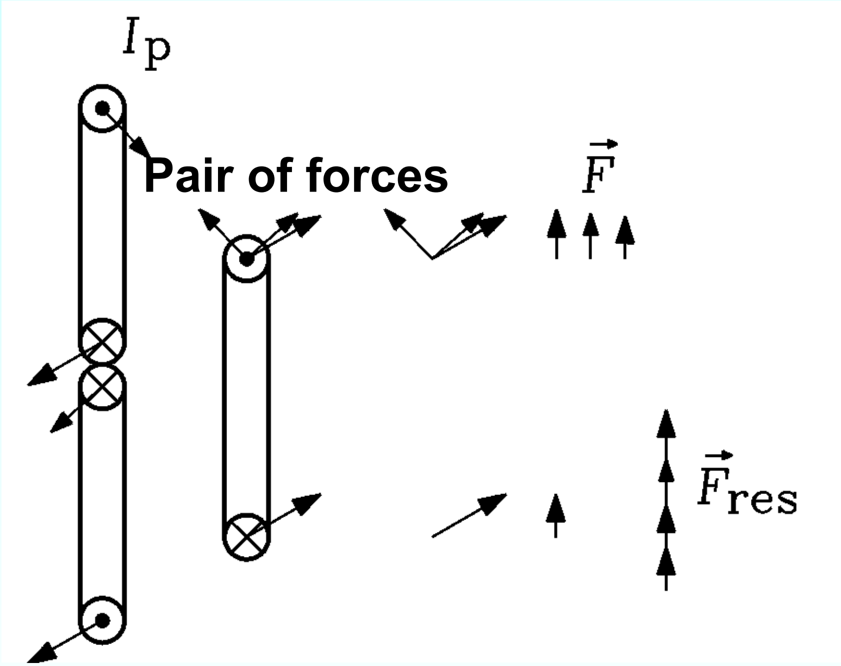

- Levitation: Vehicle is lowered below symmetry axis by the distance $-\Delta x \Rightarrow$ Now a total flux linkage with the 8-coils occurs!
- The induced coil current I_p causes with B_s a levitation force F_{res}: The vehicle is levitated stable below the symmetry axis e.g. at the levitation distance $x - \Delta x = 10$ cm.

Yamanashi: Generation of guidance force (1)

Transversal flux linkage zero in the connected coil pair, current I_p = 0

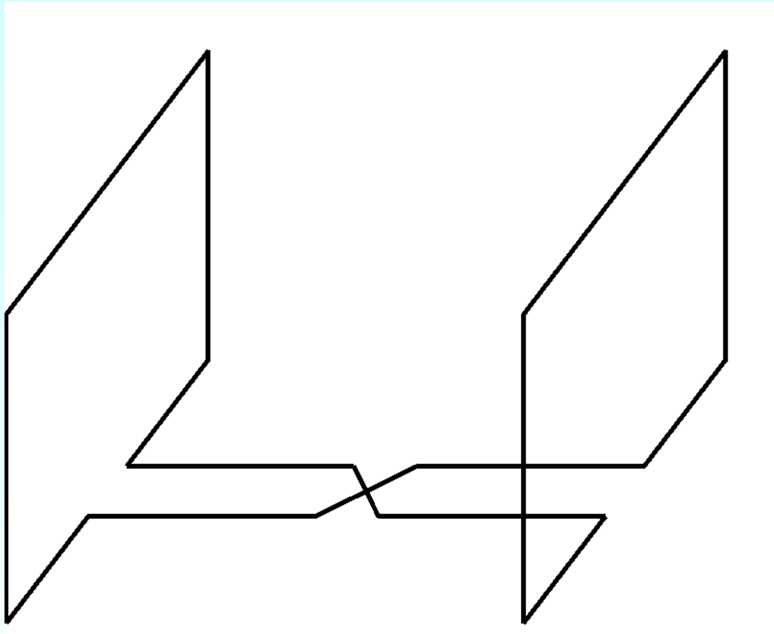

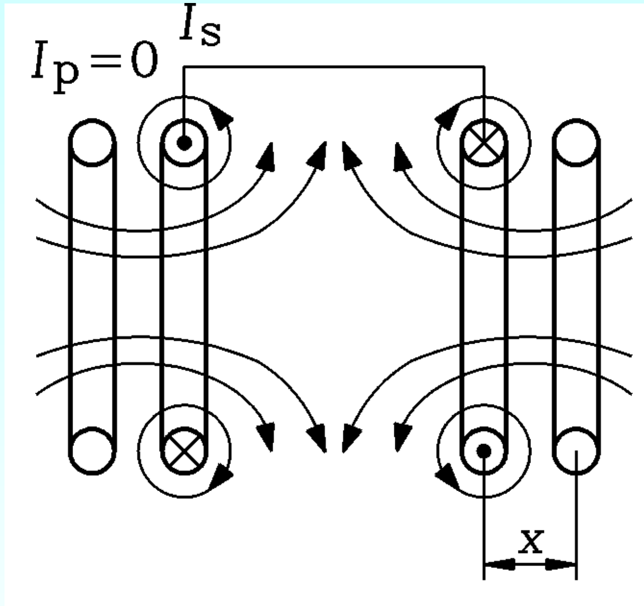

- Two Aluminum side coils are crosswise connected and short-circuited to act as guidance coils
- Transversal "Zero flux"-condition: If the vehicle is positioned in the centre between the 2 side coils, due to symmetry the total flux linkage of a coil pair is zero = no voltage induction possible = no current flow = no guidance force

Yamanashi: Generation of guidance force (2)

Flux linkage occurs: dB_p/d*t* causes current flow I_p

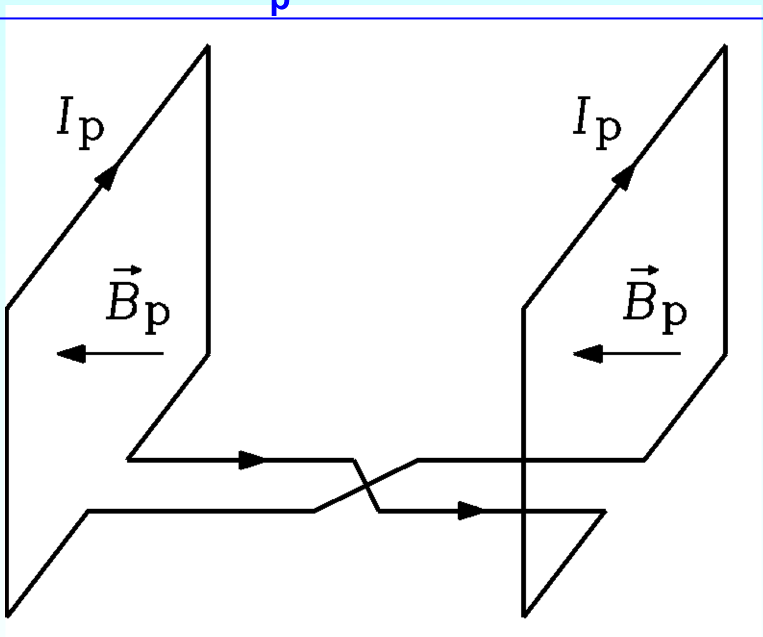

Current I_p → Guidance force F_{res}

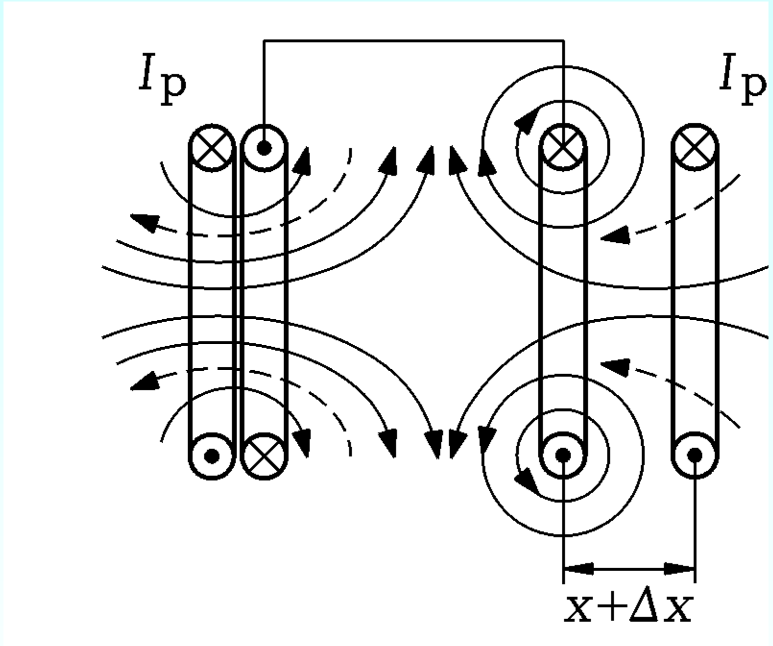

- If the vehicle is displaced laterally by Δx, the flux linkage of the DC superconducting vehicle coils with the left and right track side coil is different. A flux linkage occurs.

- The moving vehicle coils cause dΦ_p/d*t* ⇒ A voltage is induced in the track coils ⇒ Current flow I_p causes a lateral guidance force F_{res}.

Yamanashi: Generation of guidance force (3)

Current I_p → Guidance force F_{res}

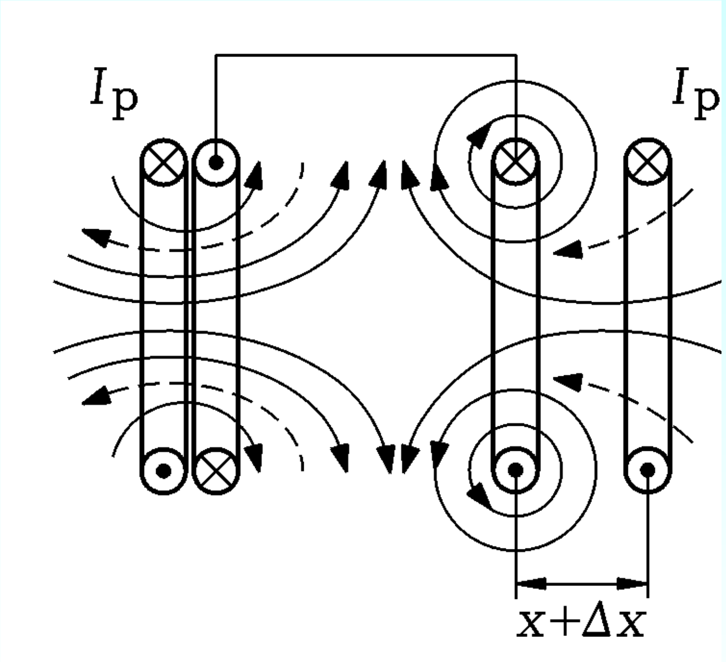

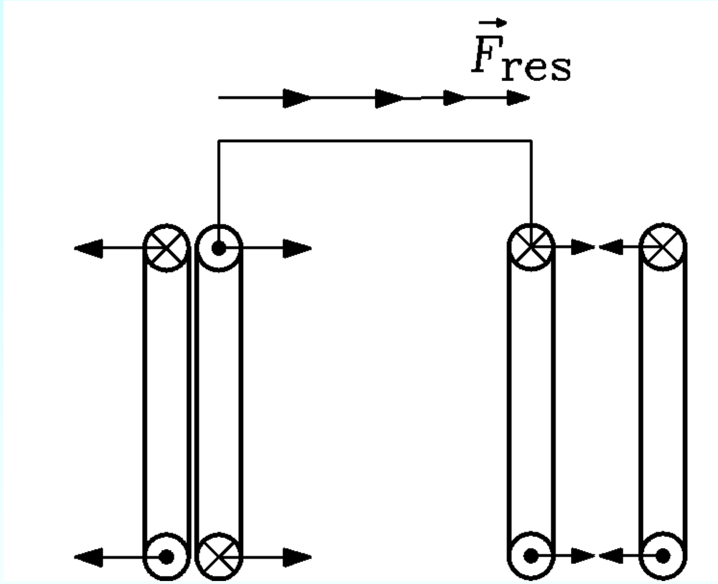

If the vehicle is displaced from the track centre to on side by Δx ⇒ A repelling guidance force F_{res} pushes the vehicle back to the centre to the track

Yamanashi high speed MAGLEV railway project

- Combination of electrical „levitation" and „guiding" coils

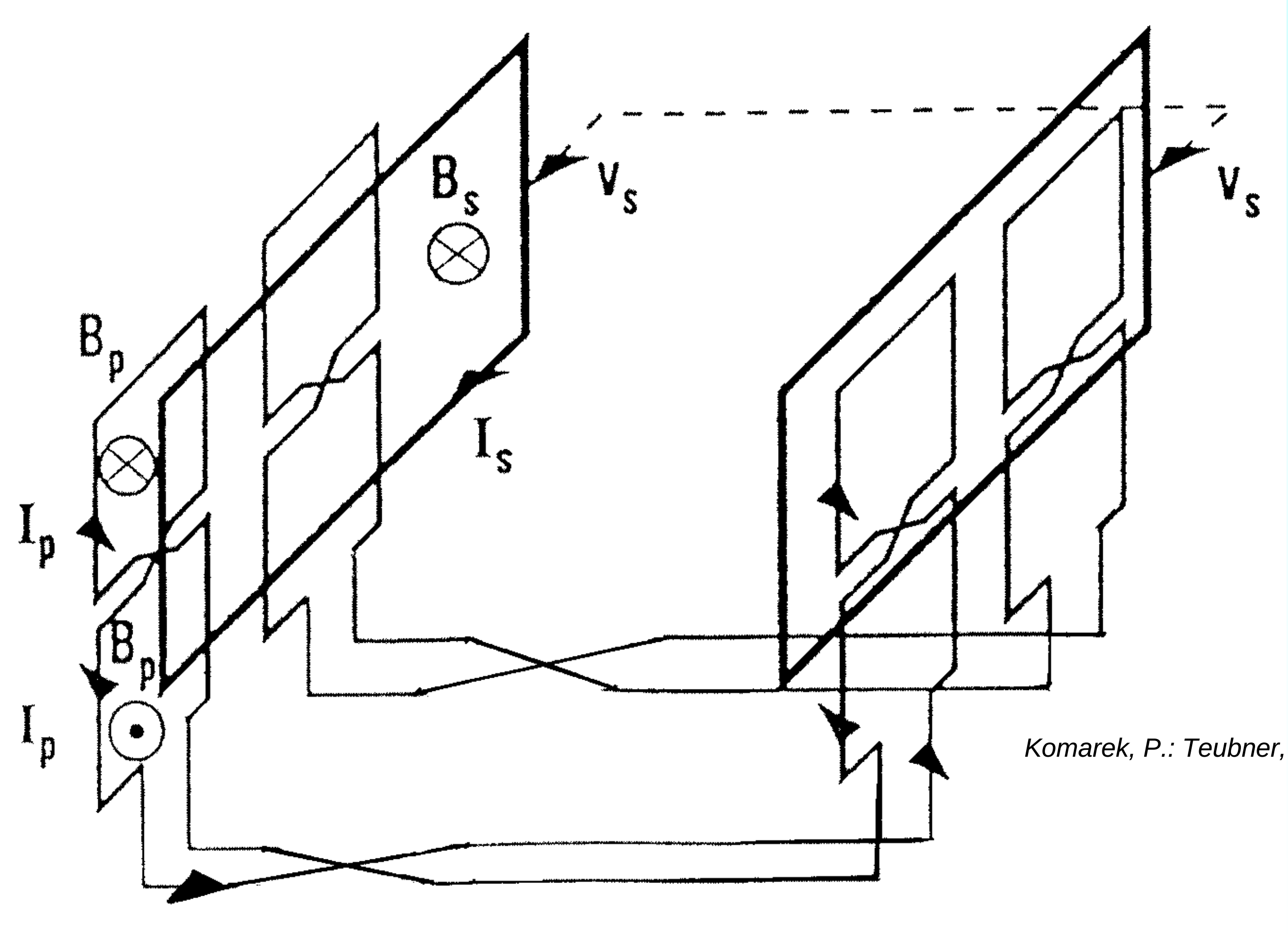

Komarek, P.: Teubner, Stuttgart, 1995

Yamanashi: Levitation and guidance coil arrangement

- Aluminum coils in the track sides for levitation and guidance at the same time: In the shape of an “8”, short-circuited and both coil sides via crossing interconnected!

a) Vertical “Zero flux position": The DC excited superconducting side coils on board of the moving vehicle are positioned exactly symmetrical to the “8-shape”: Hence the total flux linkage with the 8-shape coils is zero.

b) Transversal “Zero flux position": Left and right track-side „8-shape"-coils are crosswise connected ⇒ The total flux linkage with the coil pair is zero , if the position of the vehicle is at the track centre

- Guidance force: If the vehicle is shifted laterally to one side ⇒ A resulting flux linkage in the coil pair occurs ⇒ An induced current flow in the track coils causes a repelling force as guidance force.

Superconductor DC coils on board of the vehicle (1)

- Oval shape side coils: Coil shape (1.07 m x 0.5 m)
- Compact superconductor coil winding (1167 turns), low stabilizing Cu-matrix part:
  Cu/NbTi-ratio $\alpha = 1$:
  Allows a mass reduction to 75 kg,
  NbTi-multifilament conductor, q = 1x2.1 mm^2,
  I_s = 600 A, $I_s/q = J_s$ = 243 A/mm^2, B_s = 5.9 T
  Short circuit DC current I_s flowing in the DC superconductor coil.
  Ampere-turns: 1167 x 600 A = 770.2 kA
- Low loss on-board cryostat: Outer tank of aluminum, inner "cold" tank made of stainless austenitic steel.
  Force transfer from the DC coils via the cold tank to the outer tank via cylindrical carbon fiber-epoxy-composite tubes

Superconductor DC coils on board of the vehicle (2)

- Temperature difference: 4 K (DC coil) to 80 K at the radiation shield (made of glass fiber-epoxy composite), and from 80 K to 293 K at the outer tank: Total heat inflow via heat conduction, convection and radiation: only 5 W.
- Self-stable oscillations of the vehicle around the equilibrium position cause induced eddy currents in the Alu outer tank, which help to damp the oscillations.
- Further harmonic fields from the long stator synchronous motor also induce the Alu tank. Its shielding currents prevent a harmful penetration of these outer fields to the DC superconductor. Heat inflow to the DC superconducting coils due to the eddy current losses: 3 W !
- On-board integrated cryogenic generation of LHeI: for the cooling of the coils: 5+3 = 8 W heat transfer necessary at 4.4 K. In addition on top of the cryostat a LHeI-reservoir and a LN_2-reservoir for the radiation shield are used.

Superconductor DC coils on board of the vehicle (3)

- Heat in-flow: 5 W, additional heat in-flow due to eddy current losses in the outer tank during vehicle movement: 3 W
- On-board refrigerator for LHeI-generation to remove max. 8 W of heat power at 4.5 K from the LTSC coils (electrical nominal power of the refrigerator: 8 kW)
- Radiation shield cooled with LN_2 at 77 K … 80 K
- LTSC-DC-coils are "charged" with DC exciting current (700 kA Ampere-turns) in the MAGLEV depot – the coils are short-circuited and operate with circulating zero-loss DC current

Yamanashi-coil system

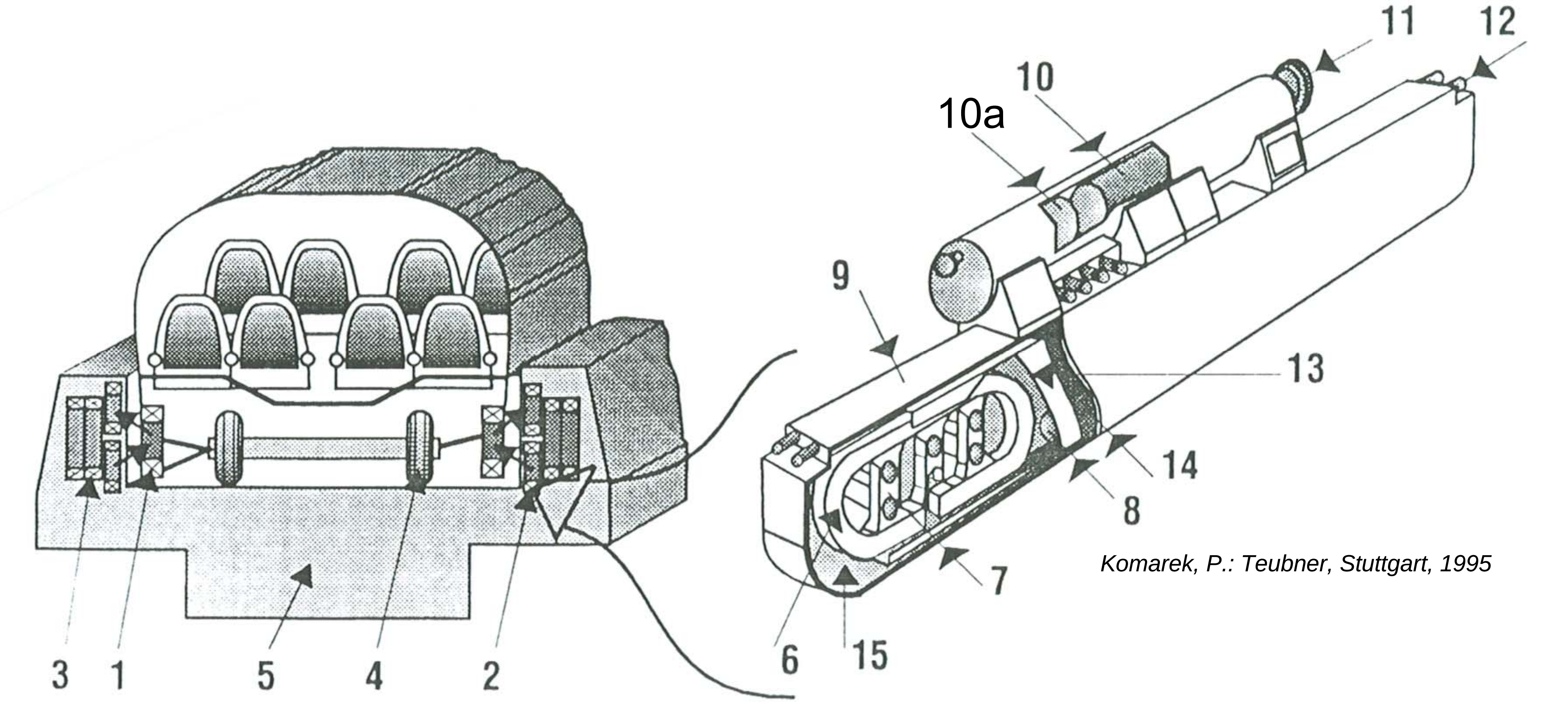

Komarek, P.: Teubner, Stuttgart, 1995

1: Superconducting magnets, 2: Levitation coils („8-shaped"-coils), 3: Synchronous motor two-layer linear drive coil, 4: wheels for accel./breaking, 5: track, 6: supercond. coils, 7: force transmission cylinder, 8: superconducting short-circuit switch for cycling DC current flow, 9: cryostat, 10: LHeI-Tank, 10a: LN_2-tank, 11: small on-board LHeI-cooling system, 12: current feeder to coil, 13: radiation shield, 14: Super isolation against heat in-flow, 15: Vacuum

Superconducting magnets of testing vehicle for EDL

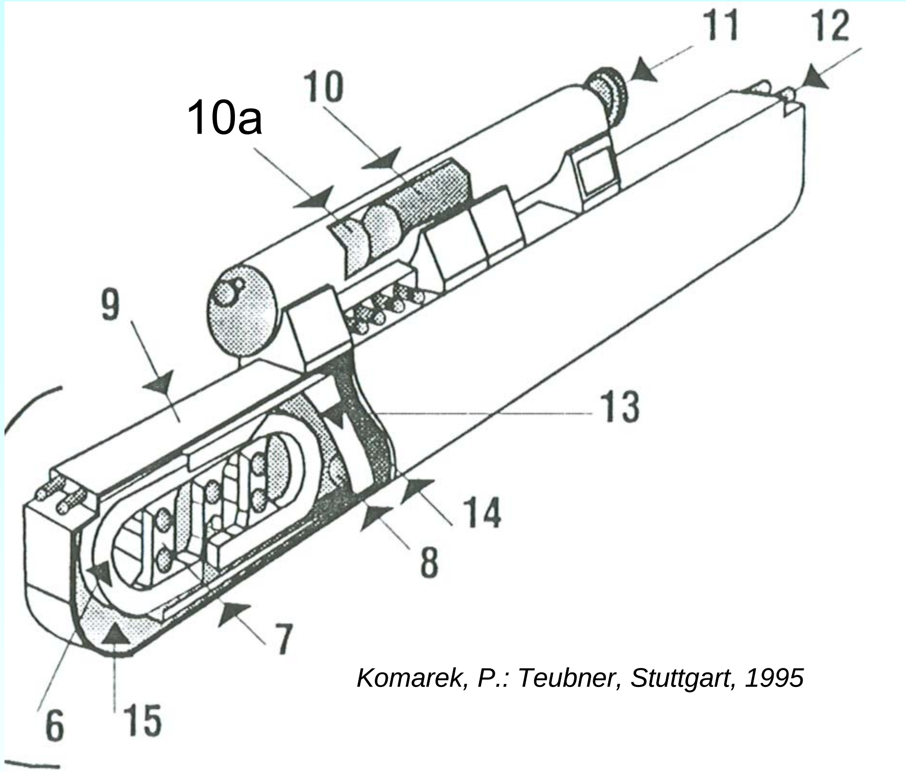

6: Superconductor coil, 7: force transmission cylinder, 8: superconducting short-circuit switch for circulating DC current operation, 9: Cryostat, 10: LHeI-Tank, 10a: LN2-tank, 11: small on-board cooling system, 12: current feeder for DC coils, 13: radiation shield, 14: super isolation against heat in-flow, 15: vacuum

Cryostat on-board of the *Yamanashi* vehicle

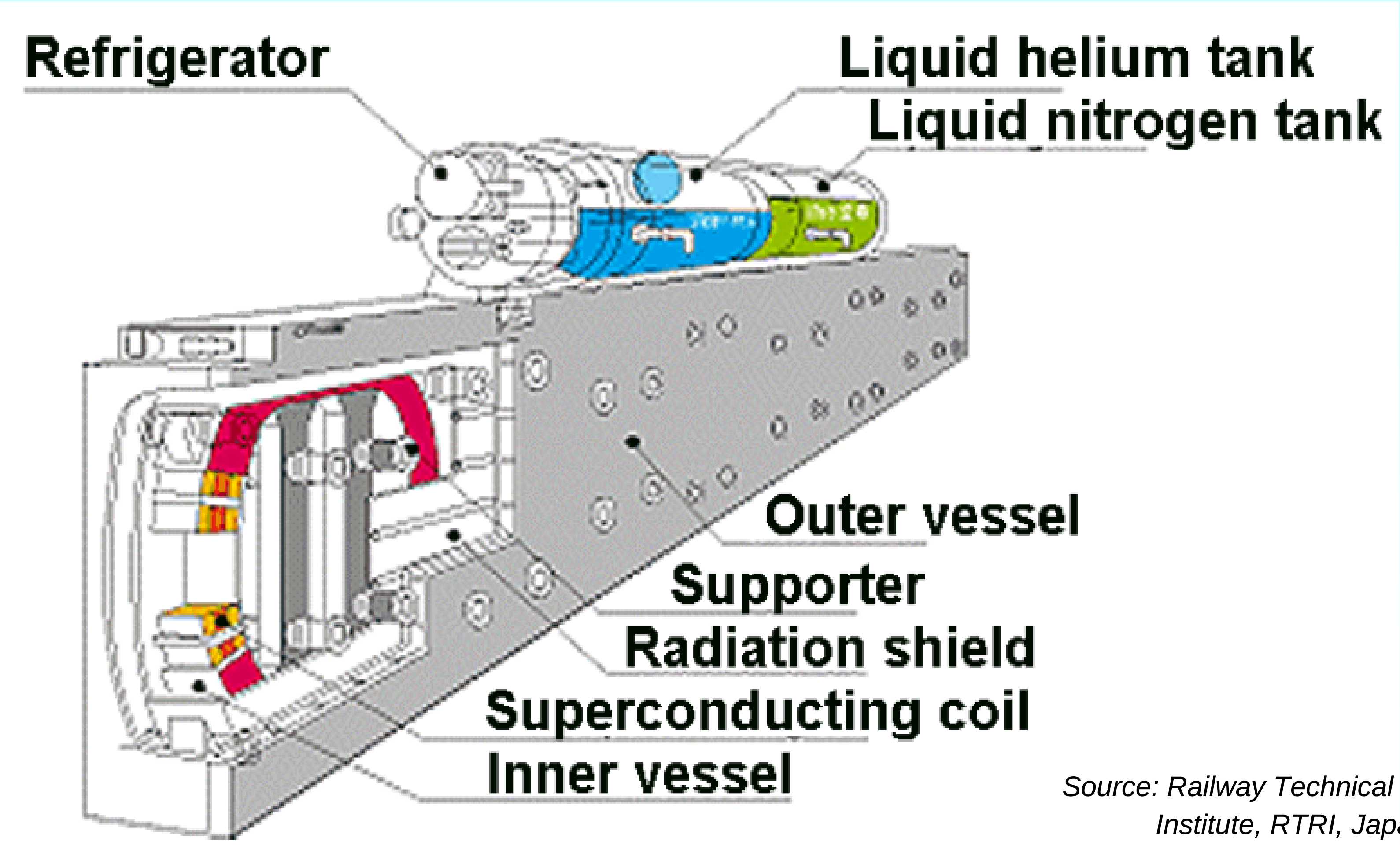

Source: Railway Technical Research Institute, RTRI, Japan

Yamanashi – Ironless coil system

- The integer ratio of linear motor coils span and of the levitation coil span (here: 4) gives no flux linkage from the levitation winding to the motor winding!

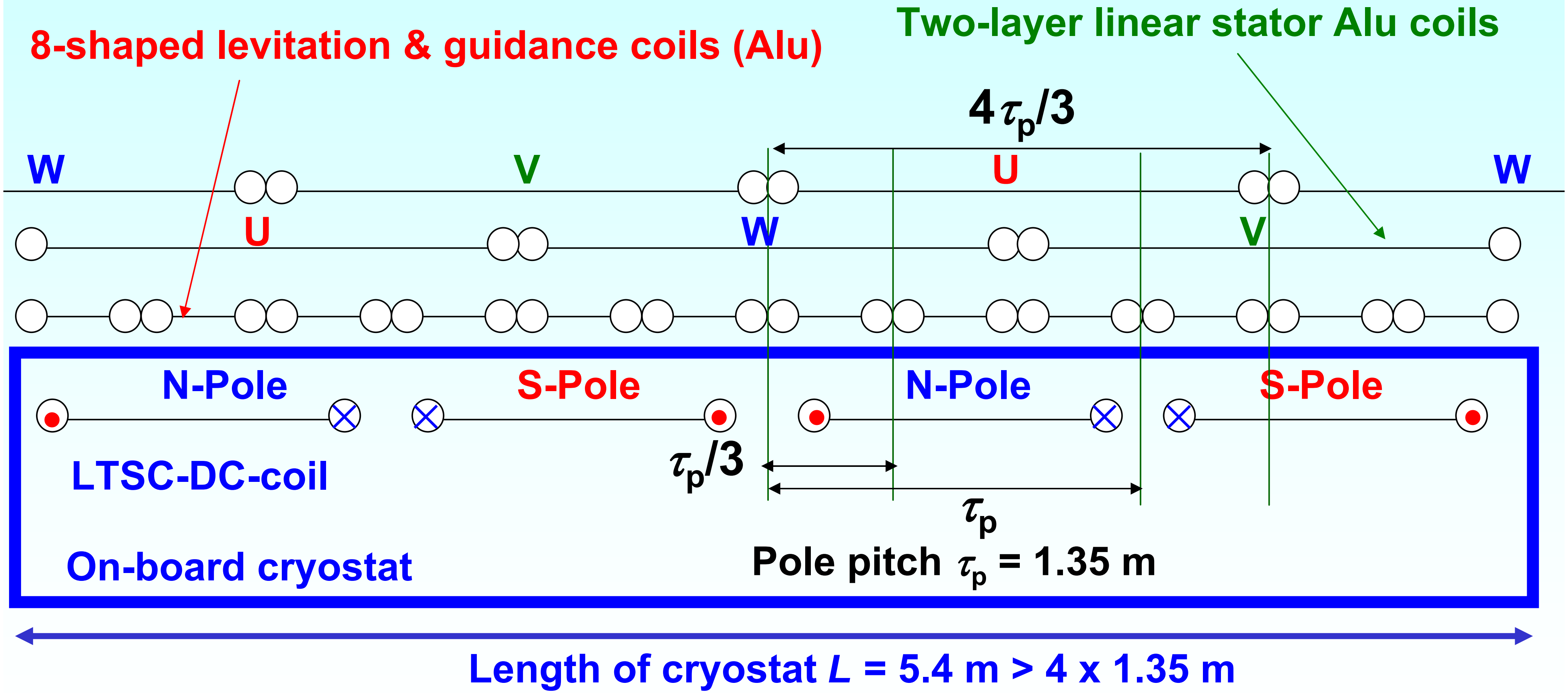

Yamanashi track coils

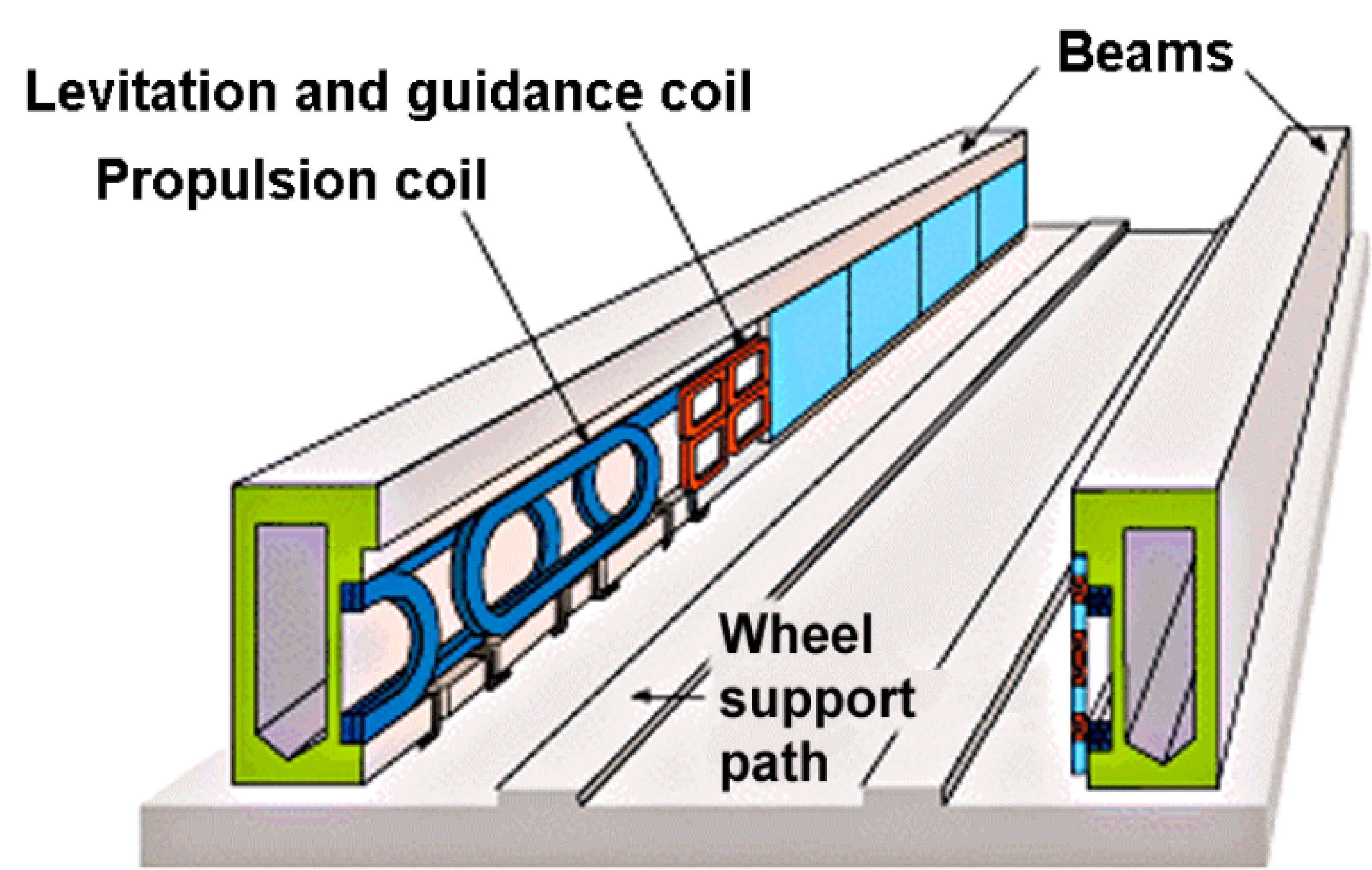

Source: Railway Technical Research Institute, RTRI, Japan

Yamanashi track

Source: Railway Technical Research Institute, RTRI, Japan

Yamanashi – Levitation force

- Two cryostats (left & right) on-board of the vehicle
- Four LTSC-DC-Coils per cryostat
- Dimensions: L x H = 5.4 m x 1.175 m, mass 1.4 tons
- Levitation force per cryostat: 115.5 kN at 23 mm height reduction from the "zero flux position" (nearly constant above 150 km/h), 220 kN at 43 mm height reduction.
- Levitation force due to interaction with 3 „8-shaped" track coils per one LTSC-DC coil: in total 4 x 3 = 12 "8-shaped" coils = 220/12 = 9.6 kN levitation force per „8-shaped"-coil

Yamanashi track coils

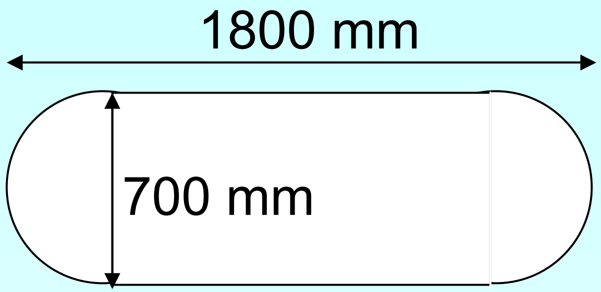

Aluminum stator coils of the synchronous long stator linear motor, two-layer winding

23 Turns per coil for lower layer coils

27 Turns per coil for upper layer coils. Due to the increased distance of the upper layer from the vehicle higher Ampere-turns are necessary for the same flux density at the vehicle DC coils

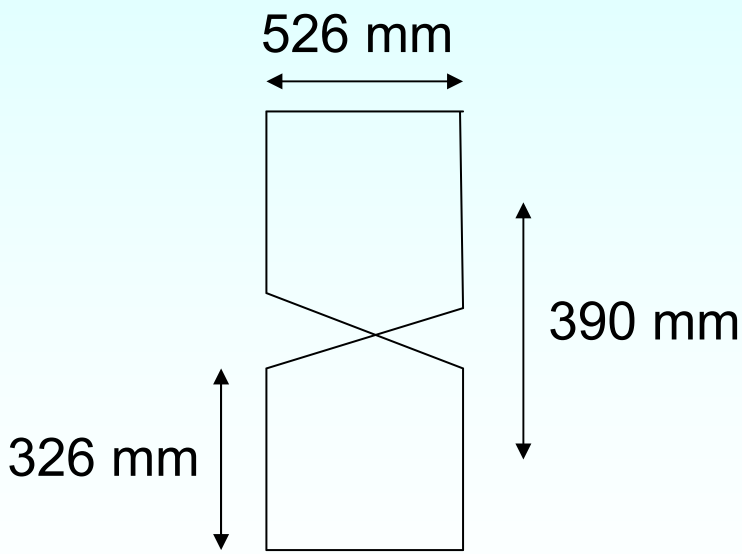

Aluminum „8-shaped" levitation & guidance coils

24 Turns per coils

Forces per 4 DC-coils at 20 mm displacement from the "zero flux" position (above ca. 150 km/h constant):

Force:	vertical: 100 kN,	lateral: 30 kN
Induced current I_p (rms):	750 A	300 A

Yamanashi - Synchronous long stator linear motor

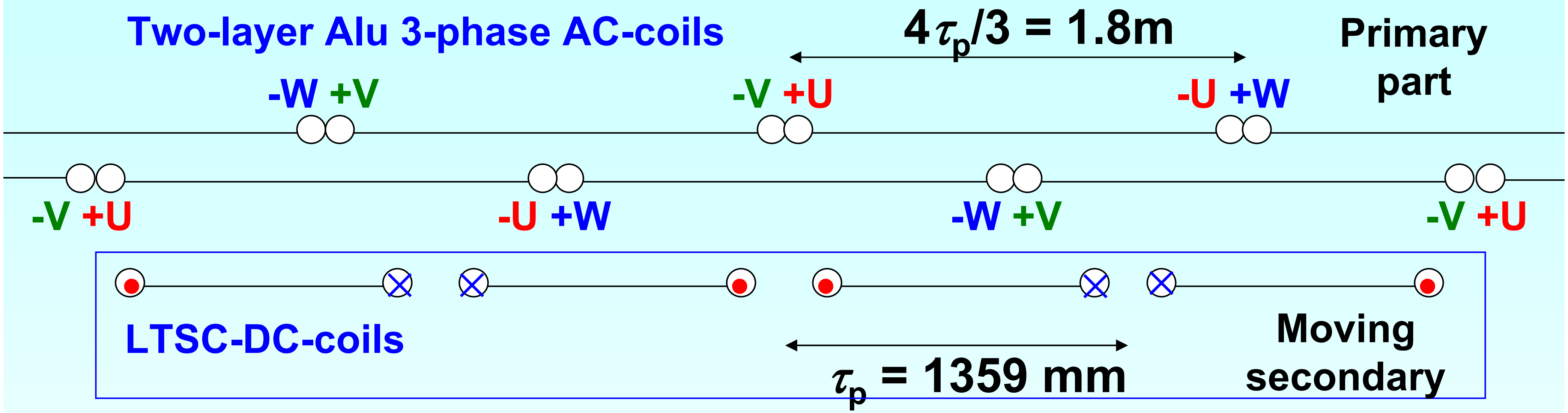

Primary: Winding scheme

$2\tau_p$

+U	+V	+W	+U	+V	+W	+U
-V	-W	-U	-V	-W	-U	-V

$W = 4\tau_p/3$

Result:

Two-layer phase belt with 3 zones per pole pair, coils over-pitched by 133%

Yamanashi - Synchronous long stator phase belt diagram

Two-layer long stator with Alu coils

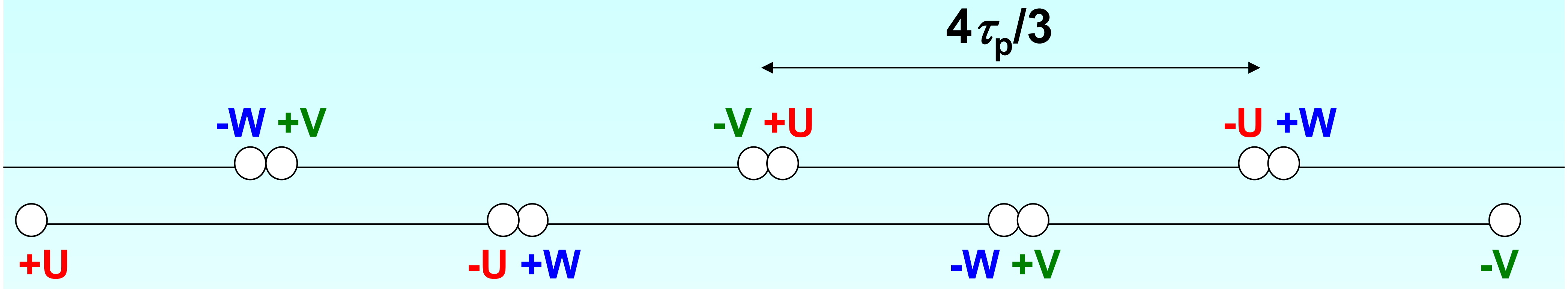

+U	+V	+W	+U	+V	+W	+U
-V	-W	-U	-V	-W	-U	-V

$2\tau_p$

+U	+V	+W	+U	+V	+W
−V	−W	−U	−V	−W	−U

Phase belt diagram of the three stator phases

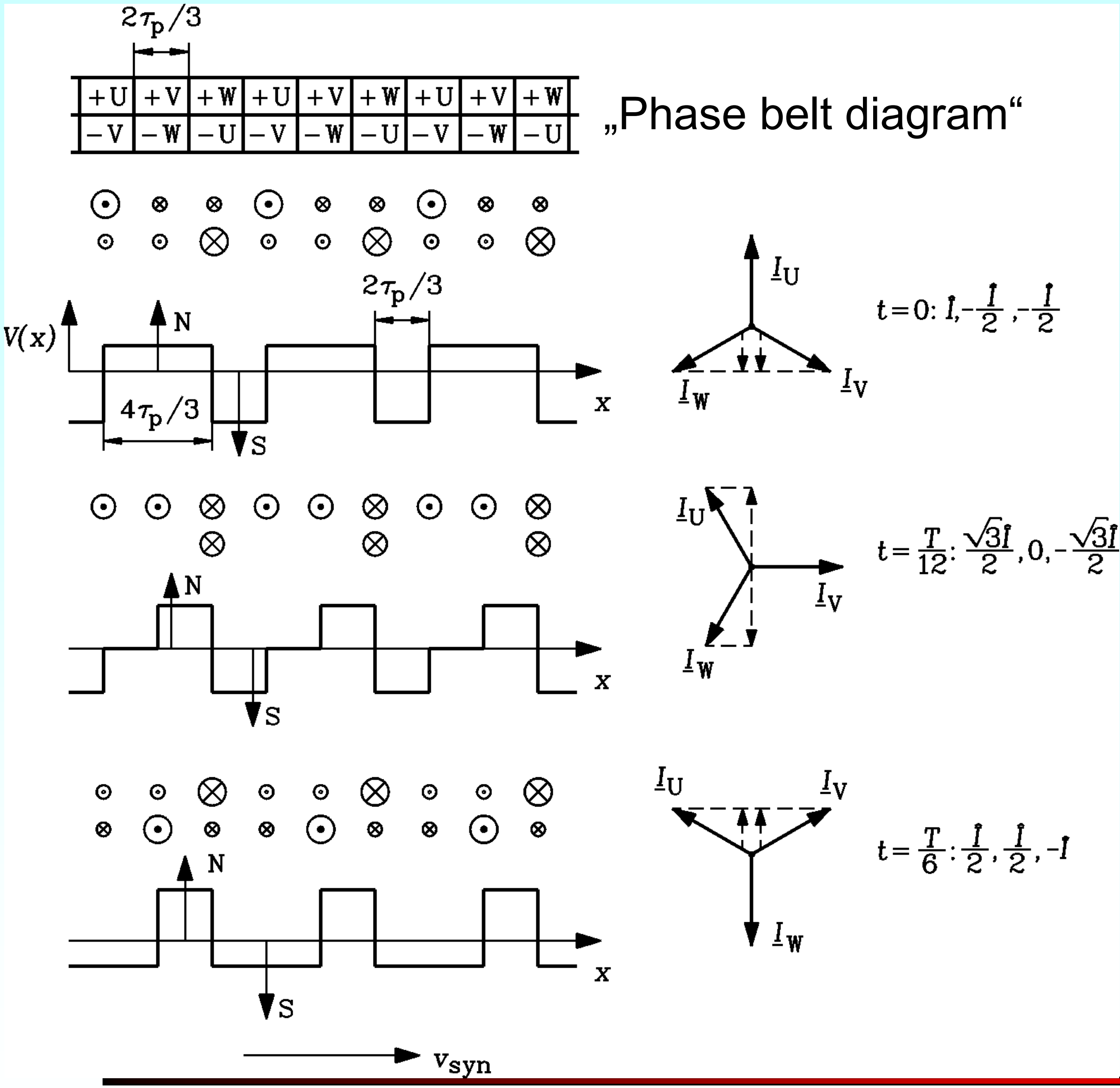

3.4 High speed trains with magnetic levitation

Yamanashi Synchronous long stator motor: Excitation of the stator travelling field

- Three zones per pole pair ⇒ N- & S-pole are not symmetrical in field distribution
⇒ *Fourier*-series of the field distribution contains harmonics with odd & even ordinal number:

$\nu = 1 + 3g$, $g = 0, \pm 1, \pm 2, \ldots$

$\nu = 1, -2, 4, -5, 7, -8, 10, \ldots$

- Fundamental wave: $\nu = 1$ used for propulsion

Yamanashi drive system

- Synchronous motor linear drive:
  - ⇒ Three phase two-layer winding, placed behind the "8-shaped" coils, excites a travelling field to the left & ride side of the track.
  - ⇒ Superconducting DC coils on-board act as motor secondary
  - ⇒ GTO-inverter feeds stator winding with a voltage of variable frequency & fundamental amplitude by PWM
  - ⇒ High gap flux density 5 T
  - ⇒ Electro-dynamic levitation: No iron parts used in the track or in the vehicle
- High levitation distance of ca. 100 mm: necessary, because often earthquakes in *Japan* ⇒ deformations of rail track ⇒ so robust traffic system is necessary with a high clearing distance above the surface level!

Yamanashi – GTO inverter power rating

- Motor pole pitch: τ_p = 1359 mm: Maximum inverter fundamental frequency for 550 km/h max. vehicle velocity:

$$f_{max} = v_{max}/(2\tau_p) = (550/3.6)/(2\cdot 1.359) = 56\text{Hz}$$

- The propulsion power is determined at high velocity mainly by the air drag:

$$S \sim P \sim v^3$$

- *Yamanashi* Track A: 38 MVA, v_{max} = 550 km/h, f = 0 … 56 Hz
- *Yamanashi* Track B: 20 MVA, v_{max} = 450 km/h, f = 0 … 46 Hz

$$S_A/S_B = (v_{A,max}/v_{B,max})^3 = (550/450)^3 = 1.83$$

$$S_B = 20MVA \quad \Rightarrow \quad S_A = 1.83\cdot 20 = 36.6 \approx 38MVA$$

Magnetically excited vibration forces (1)

- Distribution of the secondary magnet field: m.m.f. $V_r(x) \sim B(x) \sim N \cdot i$ expanded as *Fourier*-series = Sum of harmonic field waves with only odd ordinal numbers 1,3,5,… (because secondary N- and S-pole field are symmetric) $\gamma = x\pi / \tau_p$

$$V_r(\gamma, t) = \sum_{\mu=1,3,5,...}^{\infty} \hat{V}_{r,\mu} \cos(\mu(\gamma - \omega t))$$

Field distribution of half a secondary pole:

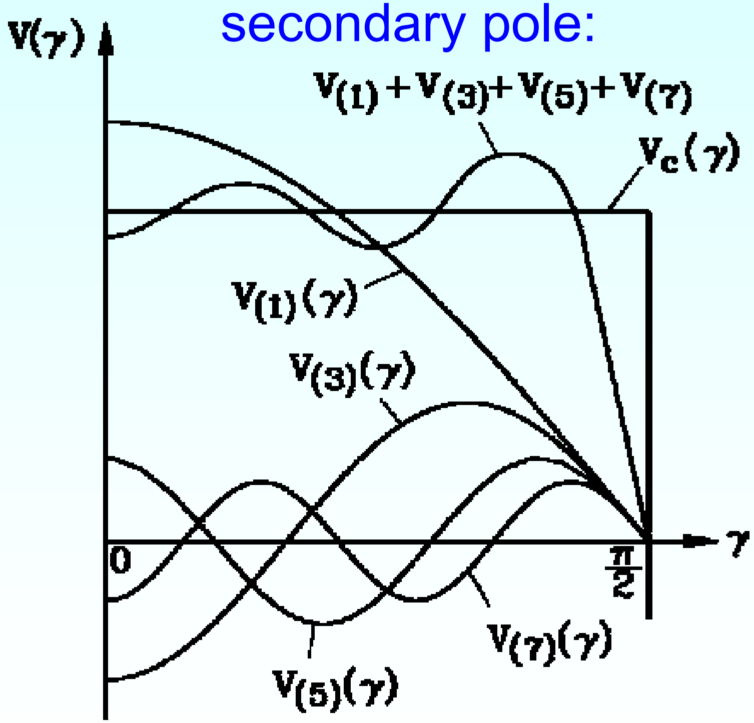

- Distribution of the primary magnetic field also expanded as *Fourier*-series: Even & odd ordinal numbers 1,-2,4,-5,7,…
  (not divisible by 3, because a 3-phase winding is used)

$$V_s(\gamma, t) = \sum_{\nu=1,-2,4,-5,7,...}^{\infty} \hat{V}_{s,\nu} \cos(\nu\gamma - \omega t)$$

- Interaction between primary and secondary harmonic field waves of the same wave length give a resulting magnetic force on the vehicle

Magnetically excited vibration forces (2)

- Frequency of the magnetic force due to interaction of primary and secondary field waves of the same wave length (= of the same ordinal number):

Fundamental waves: $\underline{\nu = 1, \mu = 1:} \; \omega_{1,1} = \omega - \omega = 0$

Constant tangential force = thrust: No force pulsation!

5. and 7. field harmonic waves are the next dominant waves:

$\underline{\nu = -5, \mu = 5:} \; \omega_{-5,5} = 5\omega - (-\omega) = 6\omega$ $\underline{\nu = 7, \mu = 7:} \; \omega_{-5,5} = 7\omega - \omega = 6\omega$

A force pulsation with 6-times fundamental frequency occurs !
At 500 km/h: Calculated force on the second LTSC-coil in the cryostat:
Force amplitude in driving direction: 880 N, lateral: 90 N, vertical: 20 N

Facit:
By sweeping the fundamental frequency between 0 … 56.6Hz (= 0 … 550 km/h), the frequency of pulsating forces on the cryostat varies between 6x(0…56) = 0 … 339.6 Hz!

Magnetically excited vibration forces (3)

- Eigen-modes of the 3D vibration of the cryostat :

  a) Torsion vibration at the natural frequency 278 Hz

  b) 2nd order flexural vibration („S-mode") with natural frequency 253 Hz

  Resonant excitation of these eigen-modes with 6-times of the fundamental frequency at

a) 450 km/h: (450/550)x339.6 = 278 Hz: Acceleration $a = d^2s/dt^2$ of vibration s: $a = 5g = 50\ \mathrm{m/s^2}$

b) 410 km/h: (410/550)x339.6 = 253 Hz: Acceleration $a = d^2s/dt^2 = 3g = 30\ \mathrm{m/s^2}$

Facit:
A damping of the vibration modes is necessary. This is accomplished by the aluminum outer containment of the cryostat: Due to the vibration it moves within the static magnetic field. Induced eddy currents generate damping reaction forces!

Magneto-static shielding

- Magneto-static shielding necessary due to the ironless coil excitation of big magnetic fields with far reaching stray fields!

  ⇒ Passenger cabin: Demand: Flux densities below 5 mT

  ⇒ Magneto-static flux density B_s via metal sheets with high permeability (e.g. Mu-metal) shielded

  ⇒ Entrance zone of the cabin in the station: also shielded with a tunnel with walls of high permeability

- Outside of the vehicle:

  In 7 m distance: 2.7 mT stray field measured!

Yamanashi-test track 18.4 km between *Tokio* and *Osaka/Japan*

Meeting ride with 1003 km/h difference velocity

Source: RTRI, Japan

Prototype vehicle of the Japanese MAGLEV train

- Operator: *Central Japan Railway Company* (*JR Tokai*): Train planned with 16 vehicles and 1000 passengers per train
- 290 km track *Nagoya-Tokyo*, velocity v_{av} = 440 km/h, travelling time ca. 40 min.

Source: RTRI, Japan & engadget.com

Road map for the construction of the high-speed *Chuo Shinkansen MAGLEV* between *Tokio* and *Osaka/Japan*

- Train speed up to v_{max} = 600 km/h, travel distance between *Osaka-Nagoya-Tokyo*: 550 km, travelling time 67 min., average speed v = 550/67 = 493 km/h
- The MAGLEV train shall relieve the over-loaded *Tokaido Shinkansen* (300 km/h)
- Project cost estimated: 9 trillion yen!, paid by Central Japanese Railway (CJR)

Compare: Cost of the high-speed railway *Tokaido Shinkansen* in 1987: 5.1 trillion yen

- Construction start: April 2014
- *First step:* Extending the test track in *Yamanashi* prefecture as part of the future track from 18.4 km to 42.2 km by 2012.
- Ordered: 14 MAGLEV vehicles Series L0, to be completed by 2015.
- 290 km track *Nagoya-Tokyo*, including the *Yamanashi* track part, shall open in 2027. The 260 km track *Osaka-Nagoya* shall open before 2045.

New technologies of electric energy converters and actuators

Summary:
Japanese electro-dynamically levitated high-speed train YAMANASHI

- Long-stator air-cored synchronous linear motors along both track sides
- Electro-dynamic levitation with moving superconducting DC coil excitation
- Short-circuited aluminum coils in 8-form shape sideways for levitation
- Large levitation air-gap to allow larger track deformations (earthquakes!)
- Magnetic shielding of cabin against DC field of car
- High speed above 500 km/h until now feasible
- Commercial use as long term planning in the next two decades

New technologies of electric energy converters and actuators

3. Magnetic bearings („magnetic levitation“)

3.5 Superconducting magnetic bearings

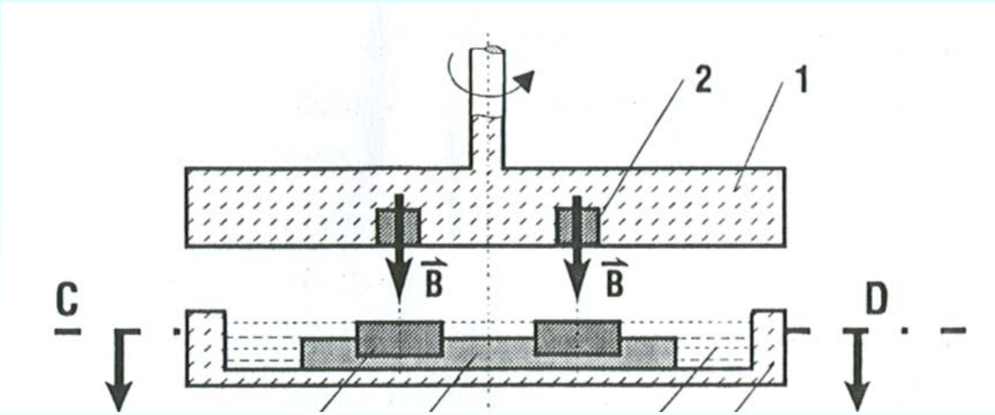

Komarek, P.:
Teubner,
Stuttgart, 1995

Superconducting magnetic bearings

- Passive magnetic bearing: melt-textured HTSC Y(123) as massif parts, operated superconducting at 77 K (with LN_2 bath cooling)
- Superconductors cooled from normal to SC state in the field of levitated permanent magnets $\Rightarrow$ at transition to HTSC-condition the magnetic flux is "frozen" inside the SC due to the *Shubnikov*-phase
- Every shifting of the magnets from the HTSC parts causes there a $d\psi/dt$: Shielding currents inside the Y(123) are generated, which cause a self-stable repulsing force on the magnets, which acts as a levitation force
- If the permanent magnet arrangement is rotation-symmetrical, then a rotation of the magnets causes no change of field inside Y(123), so no losses occur.
- *Shubnikov*-phase is a diamagnetic state: $0 < \mu_r < 1$, with typically $\mu_r = 0.5$: So the *Earnshaw* –Theorem does not apply.

Facit: A passive self-stable magnetic bearing without any need for control can be designed with superconductors.

„Freezing“ of PM-field in HTSC

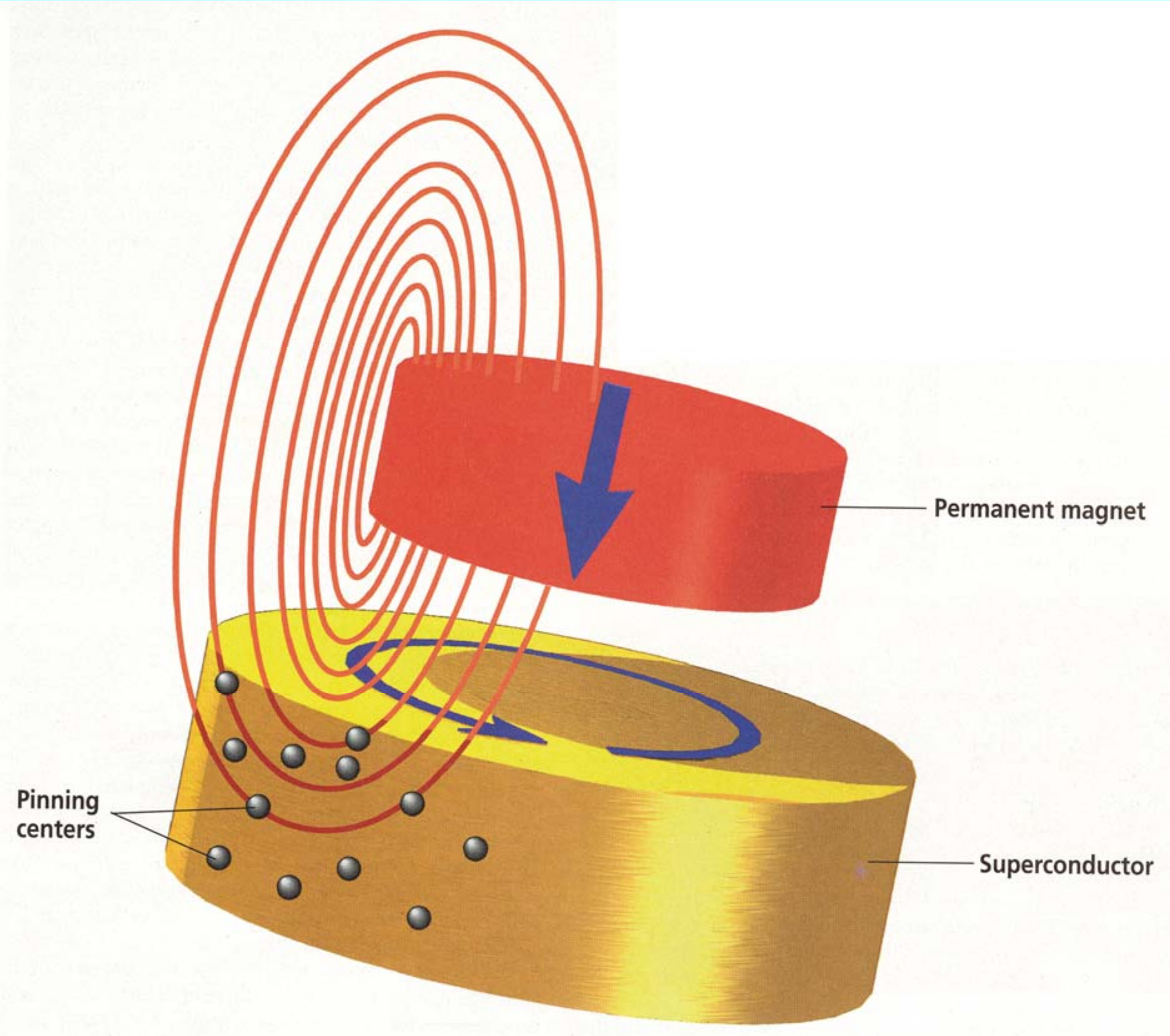

Field of the permanent magnet is “caught” at the pinning-centers of the bulk YBCO-superconductor in the *Shubnikov*-phase.

Source: IEEE PES Magazine

Principle of superconducting levitation

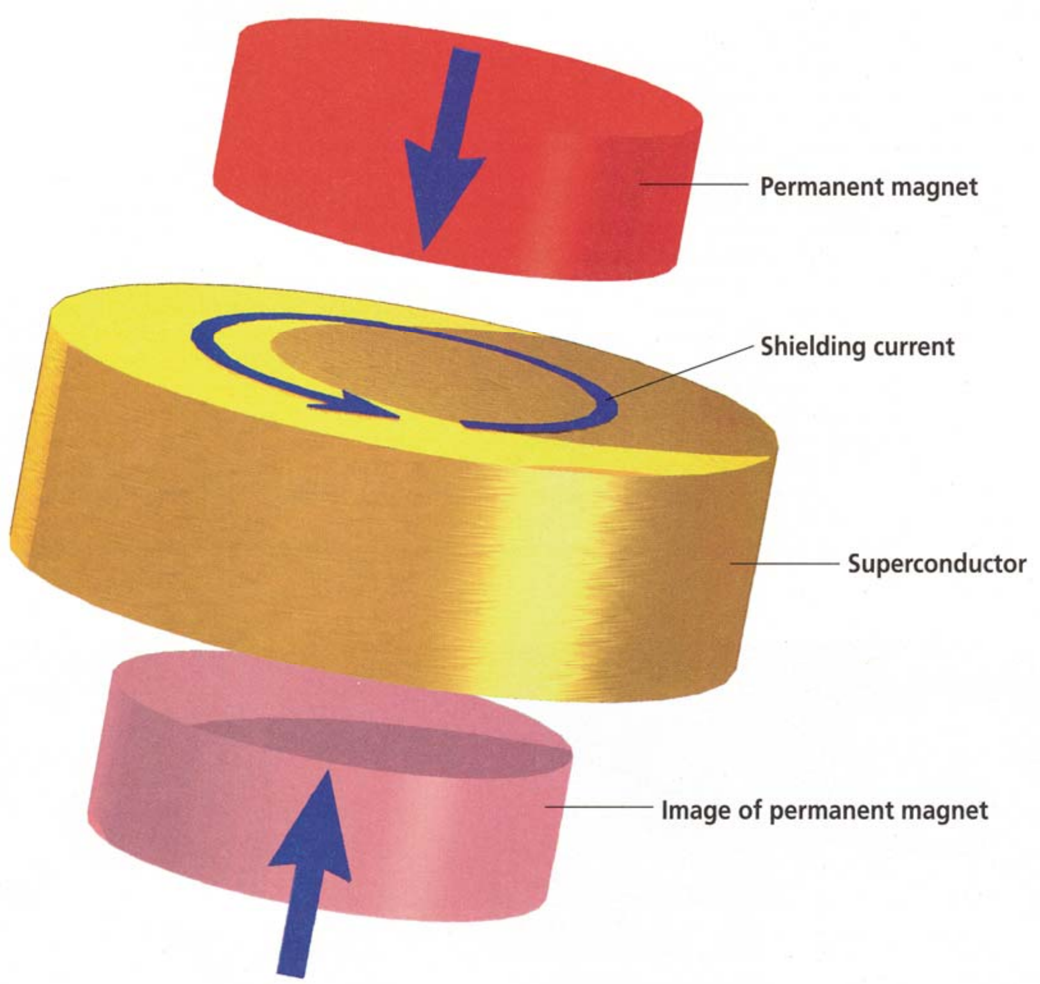

Moving of the frozen PM field in the HTSC causes a shielding current in the HTSC. These currents create an additional magnetic field, that has the same property like that of a „mirrored“ permanent magnet (“Image”), and is creating the self-stable repulsing force as a levitation force.

Source: IEEE PES Magazine

Passive magnetic HTSC-bearing

1: Flywheel as application

2: Axially magnetized ring from rare earth permanent magnet-material, NdFeB or SmCo, above a ring of disc YBCO

3: Massif HTSC as discs

4: Non-magnetic, non-conductive support of the HTSC

5: LN_2 bath cooling

6: Thermally insulated tub

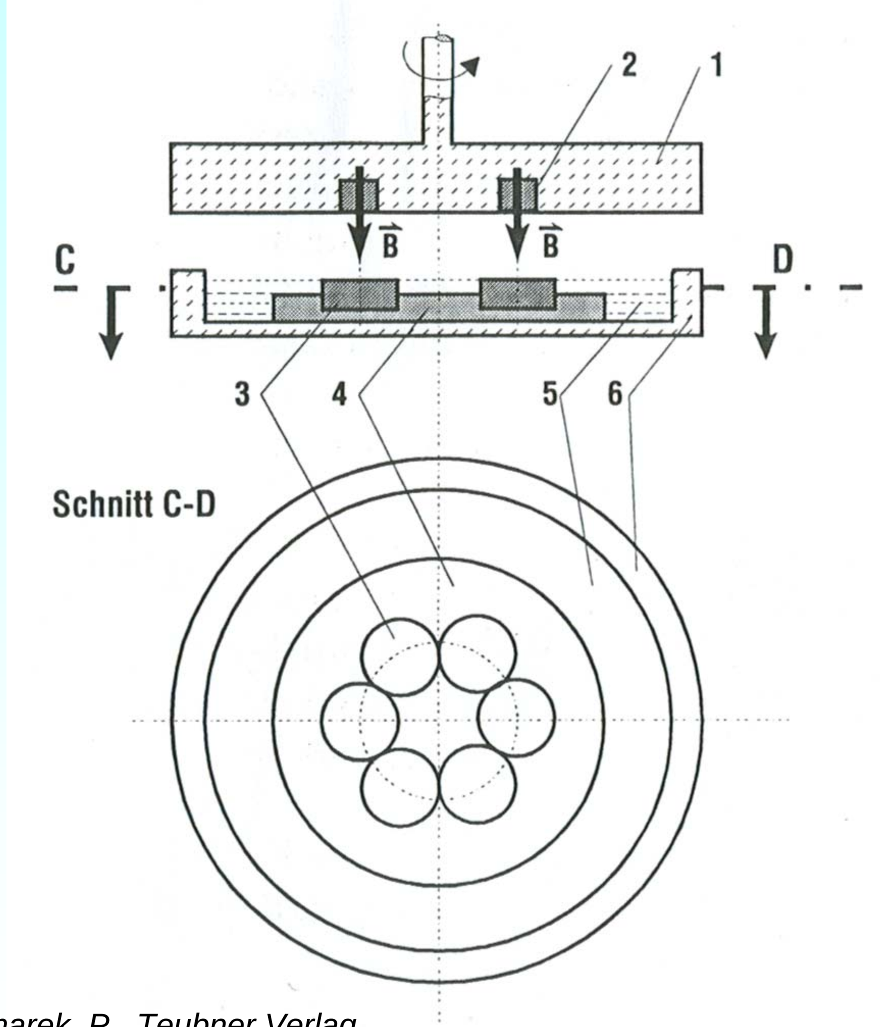

Source: Komarek, P., Teubner Verlag

Magnetic levitation force *F*

- Levitation force is proportional to the shielding current in the HTSC ⇒ proportional to the frozen magnetization *M* in the volume *V* and the change rate of the field, when moving the magnets. This corresponds to the space gradient ("grad") of the PM-field $H_M = B_M/\mu_0$ outside of the magnet.

$$\vec{F} \sim V \cdot (\vec{M} \cdot grad) \cdot \vec{H}_M$$

- Magnetization *M* proportional to shielding ring current in HTSC –volume

⇒ prop. to critical current density J_{c2} & diameter *D* of current path, because:

⇒ Magnetic momentum *m* of ring current (surface $A = D^2\pi/4$)

⇒ $\vec{m} = I \cdot (D^2\pi/4) \cdot \vec{e}_A$ (unity vector $\vec{e}_A$ vertical on *A*, right hand rule !)

⇒ HTSC volume $V = (D^2\pi/4) \cdot l$, disc height *l*

⇒ Magnetization $\vec{M} = \sum_i \vec{m}_i / V$

⇒ *Bean*-Model: Ring current covers penetration depth *x*: $I = J_{c2} \cdot x \cdot l$.

$M = m/V = J_{C2} xl \cdot (D^2\pi/4)/V = J_{c2} \cdot x$ **is maximum at *x* = *D*/2:** $M \sim J_{c2} \cdot D$

Features of HTSC magnetic bearings

- **Specific bearing forces** *f* = 5 ... 10 N/cm^2
  Bearing stiffness 10 ... 50 N/mm
- **Compare: Conventional magnetic bearing:** *f* = 30 ... 60 N/cm^2
  Dynamic bearing stiffness depends on control parameters
- **Losses in** HTSC-bearings are low: "equivalent" friction number $\mu = 10^{-6}$
  Conventional roller bearing: μ = ca. 0.001
  Active controlled magnetic bearing: $\mu = 10^{-5}$.
  Hence: HTSC-bearing good for **fly-wheel storage systems!**
- **Problem: Fissures in HTSC-volume body** due to brittle material may occur: Shielding current path interrupted. Ring current flows on a smaller diameter *D* $\Rightarrow$ Magnetic momentum *M* is reduced, and also levitation force *F*
- **At the moment**: YBCO bodies smaller than 10 cm side length; above that danger of cracks!

Features of a flywheel storage

- **Stored kinetic energy** (with polar momentum of inertia *J*): $W_{kin} = J\dfrac{(2\pi n)^2}{2}$
- **Centrifugal mass as rotation cylinder** (density ρ, height *L*, radius *R*, mass *m*)

$$J = m \cdot R^2 / 2 = \rho \cdot \frac{\pi}{2} \cdot L \cdot R^4$$ "equivalent inertia radius": $i = R/\sqrt{2}$

- **Energy density**:

$$w = W/m = \frac{J \cdot (2\pi n)^2 / 2}{m} = \frac{m \cdot (R^2/2) \cdot (2\pi n)^2 / 2}{m} = \frac{v_u^2}{4}$$

Energy density of flywheels depends only on circumference speed.

Example: **Steel disc: $v_{u,max}$ = 585 m/s: *w* = 85556 m²/s² = 25 Wh/kg.**

- **Disc with central hole** (hole radius R_i): Mass concentrated near outer rim:

$$m = \rho L \pi (R^2 - R_i^2) \qquad J = \rho L \pi (R^4 - R_i^4)/2 \qquad \boxed{w = (v_u^2/4) \cdot (1 + (R_i^2/R^2))}$$

Steel disc limit & $R_i = R$: **energy density raises to 50 Wh/kg.**
Disc material of C-fiber composite: Circumference speed v_u = ca. 1000 m/s:
***w* = ca. 200 Wh/kg**

Tensile stress σ in modern flywheels (1)

- **Centrifugal force on a mass element of the wheel:** $\Delta m = \rho \cdot L \cdot r\Delta\varphi \cdot \Delta r$
  calculated for a section $\Delta\varphi$ of the circumference & distance *r* from centre:

$$F_f = \Delta m \cdot r \cdot (2\pi n)^2$$

Resulting tangential force F_t in the material: $F_f = 2 \cdot F_t \cdot \sin(\Delta\varphi / 2) \approx F_t \cdot \Delta\varphi$

$$\sigma = \frac{F_t}{A} \approx \frac{F_f / \Delta\varphi}{L \cdot \Delta r} = \frac{(\rho L r \Delta\varphi \Delta r \cdot r \cdot (2\pi n)^2)/\Delta\varphi}{L \cdot \Delta r} = \rho \cdot r^2 \cdot (2\pi n)^2 = \rho \cdot v_u^2$$

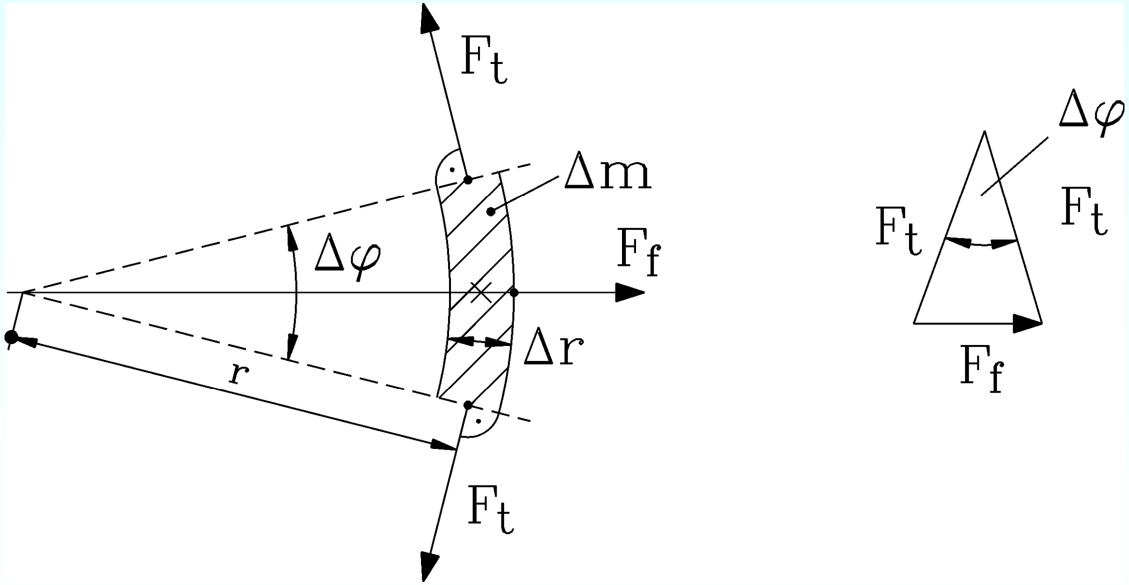

Tensile stress σ in modern flywheels (2)

- Carbon fibre composite (fibres embedded in epoxy resin matrix):
  High tensile strength of the carbon fibre e.g. 4000 N/mm². Low tensile strength of the epoxy resin, hence: resulting strength prop. to the ratio "Fibre volume/total volume": typically 0.6: σ_{max}=2400N/mm².
- With the mass density ρ = 3.5 kg/dm³ we get:

$$v_{u,\max} = \sqrt{\sigma_{\max} / \rho} = \underline{\underline{828}} \text{ m/s}$$

Compare: Active magnetic bearing rotors, manufactured from:
a) High stress dynamo sheets: σ_{max} = 500 N/mm²: ρ = 7.85 kg/dm³, $v_{u,max}$ = 250 m/s
b) Amorphous metal foils: σ_{max} = 1500 N/mm²: ρ = 7.85 kg/dm³, $v_{u,max}$ = 440 m/s

⇒ Bearing rotor diameters must be smaller than the flywheel diameter!

Friction losses in flywheels

- **Air friction losses P_{air} of a rotating cylinder in a chamber:**
  Turbulent air flow (*Reynolds* number *Re* > 1000) on cylinder surface:

$$P_{air} = 1.7 \cdot \rho_{air} \cdot n^3 \cdot (2R)^4 \cdot L \cdot \frac{1}{\mathrm{Re}^{0.15}} \qquad \mathrm{Re} = \frac{(2R) \cdot \pi \cdot n \cdot \delta}{\nu_{air}}$$

Distance between cylinder and chamber-surface: δ

- ***Example:* C-fiber composite cylinder as flywheel storage disc:**
  140°C: air density: 0.826kg/m³, kinematic viscosity $26.5 \cdot 10^{-6}$m²/s
  R = 300 mm, L = 100 mm, v_u = 600 m/s, ρ = 3500 kg/m³, δ = 100 mm

$m = \rho \cdot R^2 \pi \cdot L =$ **44 kg , *J* = 2 kgm² ,** $n = v_u / (2\pi R) =$ **318.5/s = 19100 /min**

Stored energy: *W* $= 2 \cdot (2\pi \cdot 318.5)^2 / 2 = 4004780 =$ **4 MJ**
Energy density: *w* = 4 004 780/44 = 91017 Ws/kg = 25 Wh/kg

$$\mathrm{Re} = \frac{(2 \cdot 0.3) \cdot \pi \cdot 318.5 \cdot 0.1}{26.5 \cdot 10^{-6}} = 2.26 \cdot 10^6 > 1000$$

Air friction: $P_{air} = 1.7 \cdot 0.826 \cdot 318.5^3 \cdot 0.6^4 \cdot 0.1 \cdot (2.26 \cdot 10^6)^{-0.15} = \underline{\underline{65.5}}\,\mathrm{kW}$

Loss of stored energy through friction

- *Example:* W = 4 MJ, P_{air} = 65.5 kW: Neglecting that the air friction losses decrease with n^3 at decreasing rotational speed n, the stored energy is consumed by friction after the time $T = W/P_{air}$ = 61 s (= 1 minute !).
- For using flywheels as energy storage the friction losses must be minimized.
- Hence the flywheel should rotate in vacuum. For that, magnetic bearings are the best:

a) They do not need any lubrication.
b) The gap can be evacuated between bearing stator and shaft.

- As active magnetic bearings need position sensors, controller and excitation energy for the coils, HTSC-magnet bearings are an interesting alternative.
- But then there is a need of energy for supply of cooling LN_2.

Example: Flywheel system with conventional bearings 1

Volvo/Sweden:
Car with front drive combustion engine 187 kW.

Fly wheel storage: 59 kW at 60 000/min, speed variable gear and switchable coupling to the rear axis

Switch-in above 40 km/h, braking energy is stored

Flywheel data: 20 cm diameter, carbon fibre, 6 kg (SKF)

Fuel saving (NEDC): 10%
Under "real" conditions: 20%

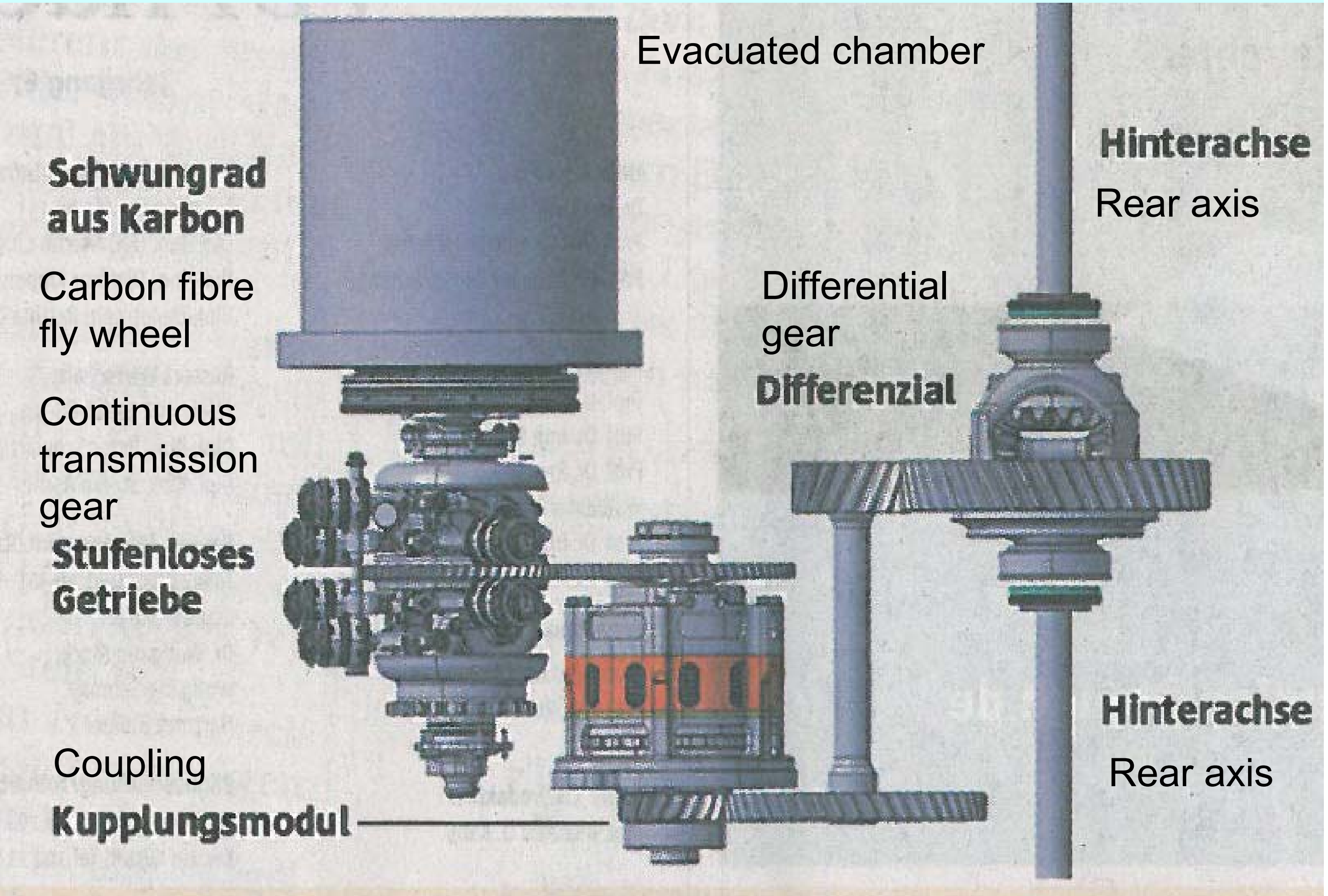

Source: Volvo, VDI-Nachrichten, 6.9.2013

Example: Flywheel system with conventional bearings 2

Mass assumed to be concentrated at the outer rim:

$$d = 0.2m \quad m = 6kg \quad J \approx m \cdot r^2 / 2$$

$$J \approx m \cdot (d/2)^2 / 2 = 6 \cdot 0.1^2 / 2 = 0.03 kg \cdot m^2$$

Stored kinetic energy:

$$W = J \cdot \Omega_m^2 / 2 =$$

$$= 0.03 \cdot (2\pi \cdot 60000/60)^2 / 2 = 592 kJ$$

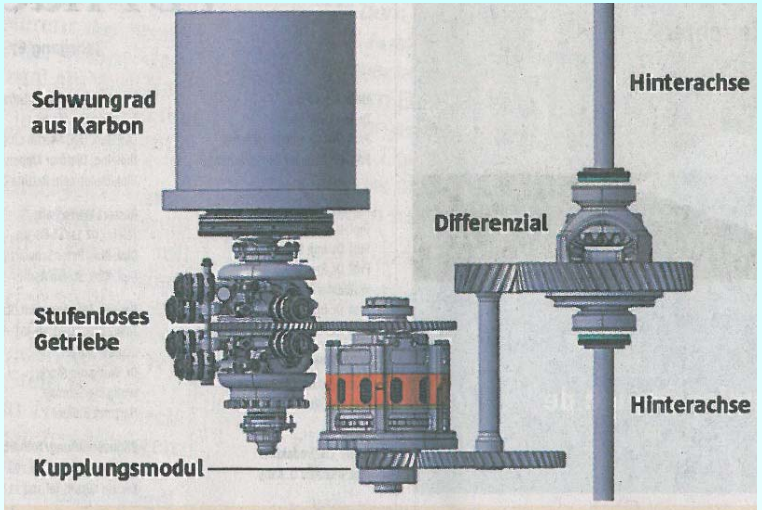

Source: Volvo, VDI-Nachrichten, 6.9.2013

***Volvo* data: Stored kinetic energy: 540 kJ, full discharge during 9.1 s:**

$$P = W / t = 540 kJ / 9.1 s = 59 kW$$

***Volvo* data: Operated partial discharge: 6 … 8 s**

Estimated friction losses: P_{fr} = 300 W: After 30 min. full discharge by friction at car stand-still or driving without braking

$$T = W / P_{fr} = 540 kJ / 0.3 kW = 1800 s = 30 \min.$$

Flywheel storage system with SC magnetic bearing

Source: IEEE PES Magazine

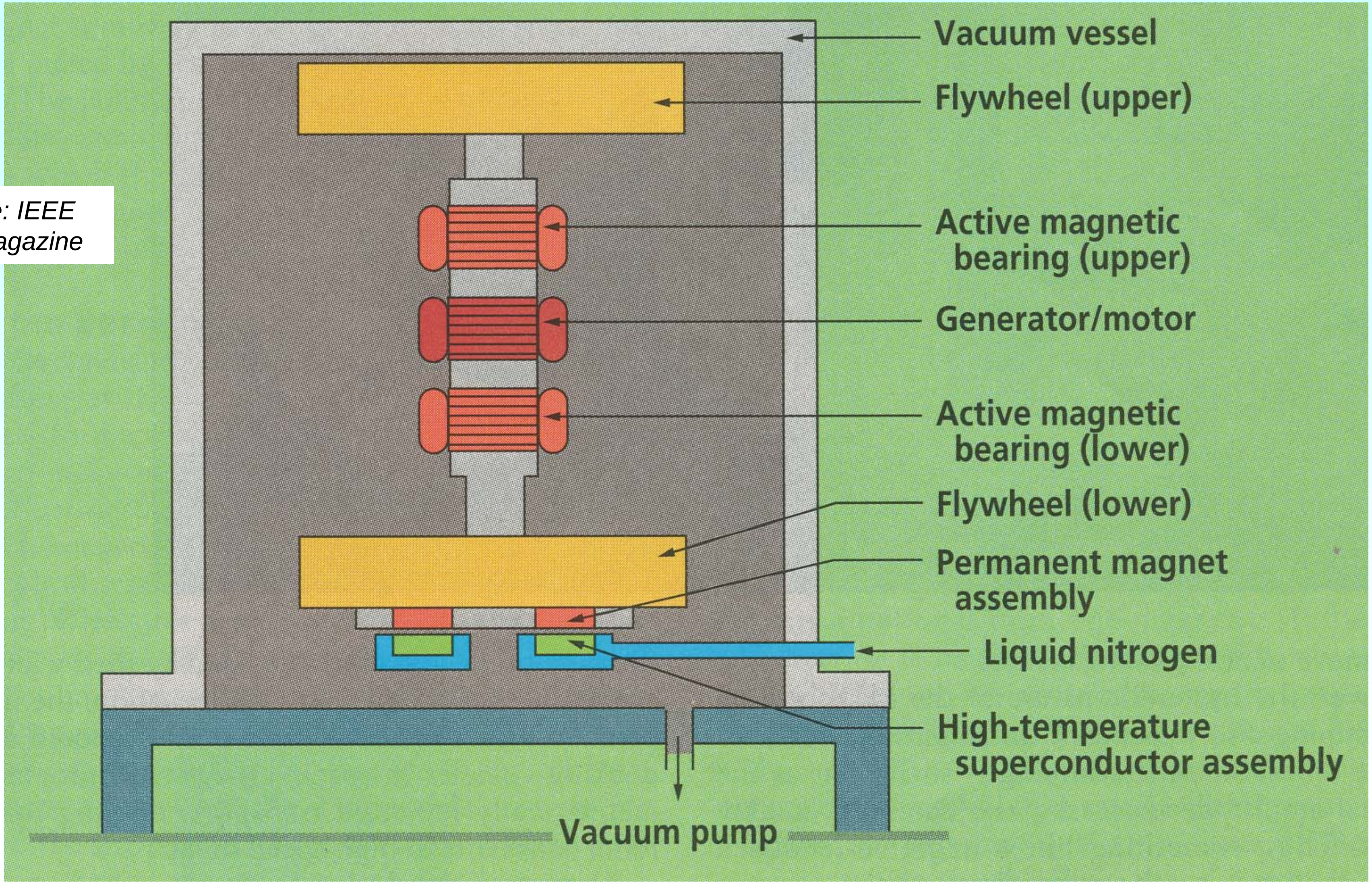

Carbon fibre composite flywheel with HTSC bearing

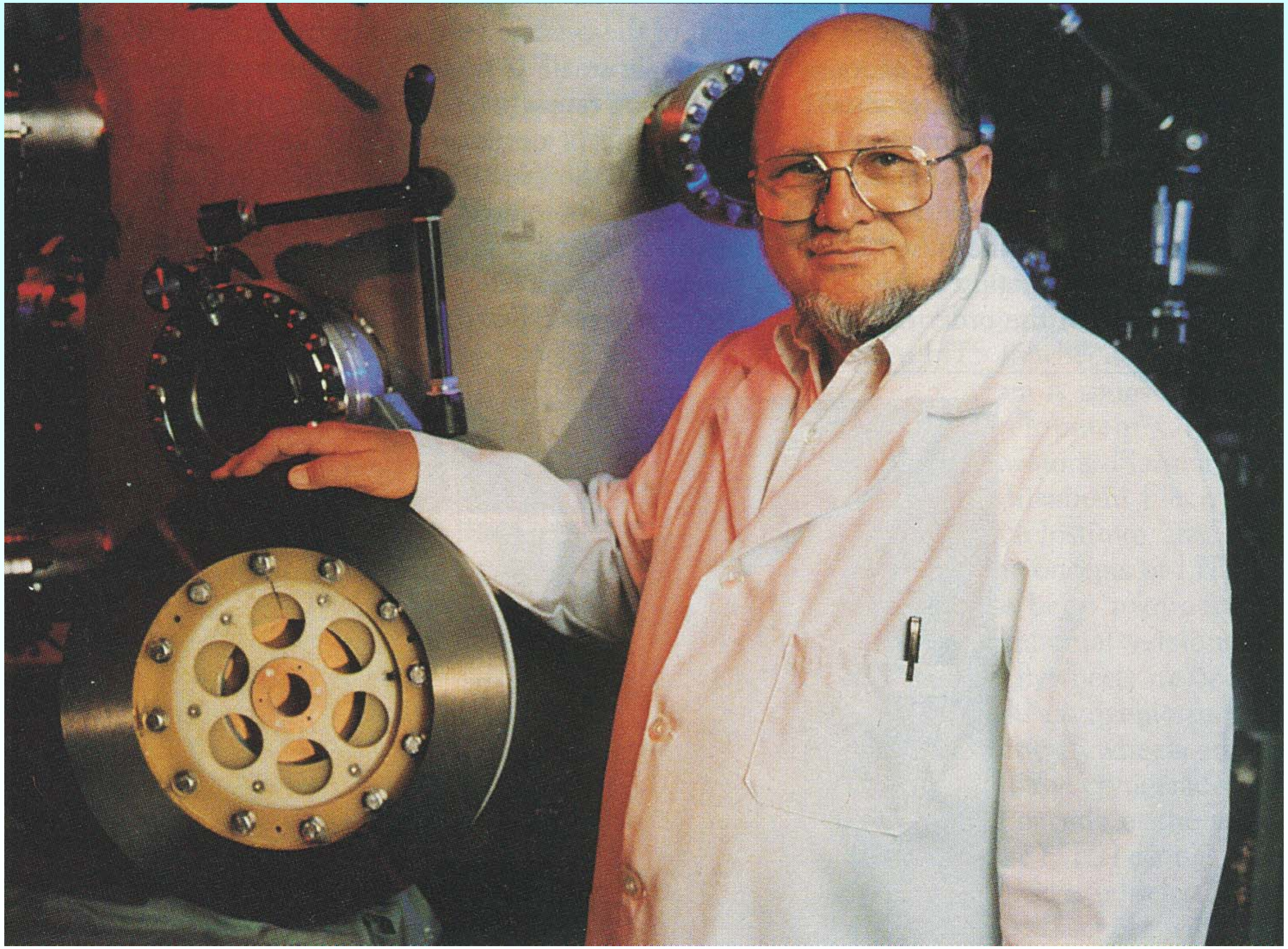

- Carbon fibre composite flywheel
- Glass fibre rotor with pick-up for 6 PM discs for HTSC Y(123)-bearing
- Generator-/Motor-flange in the centre of the glass-fibre rotor
- Background: Flywheel enclosure

Source: Argonne Nat. Lab., USA

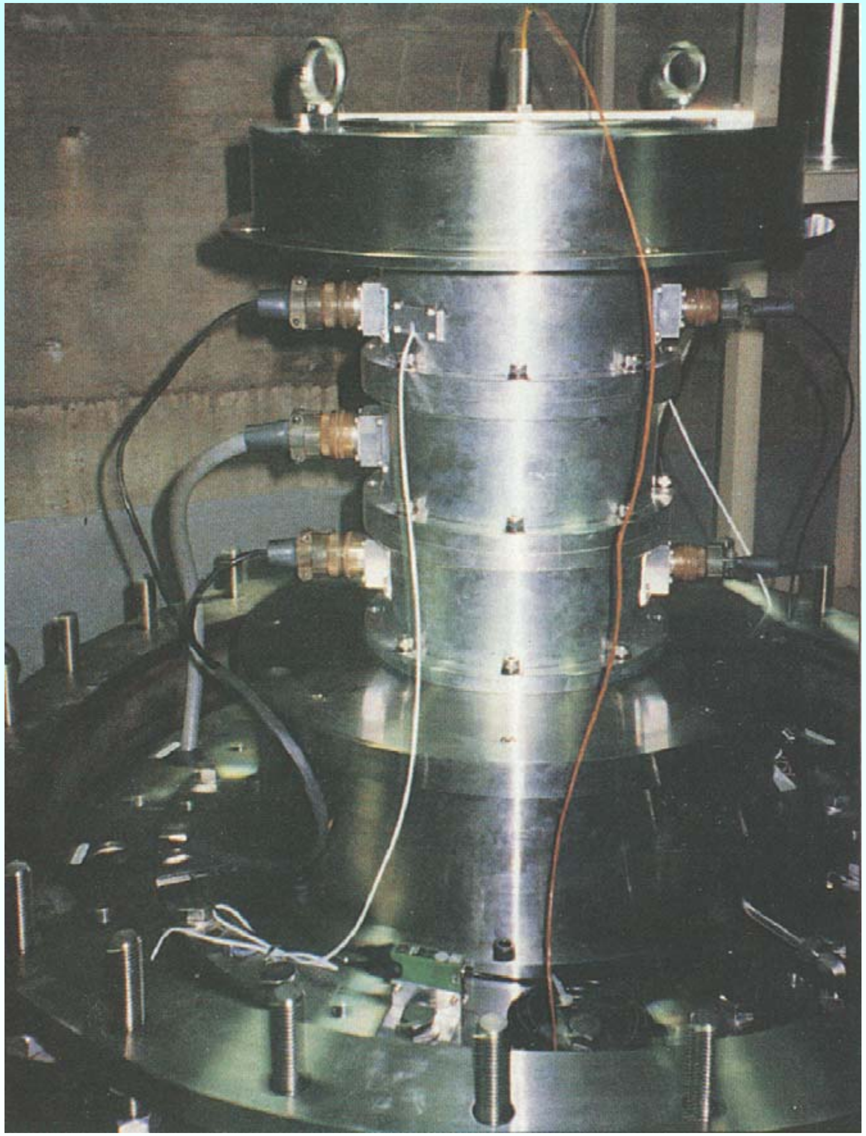

Flywheel storage with SC magnetic bearing

- Evacuated flywheel enclosure with

a) Motor-Generator

b) HTSC-bearing Y(123) with LN_2-cooling

c) Carbon fibre composite flywheel

Source: Argonne Nat. Lab., USA

Prototype of a flywheel storage system with HTSC magnetic bearings

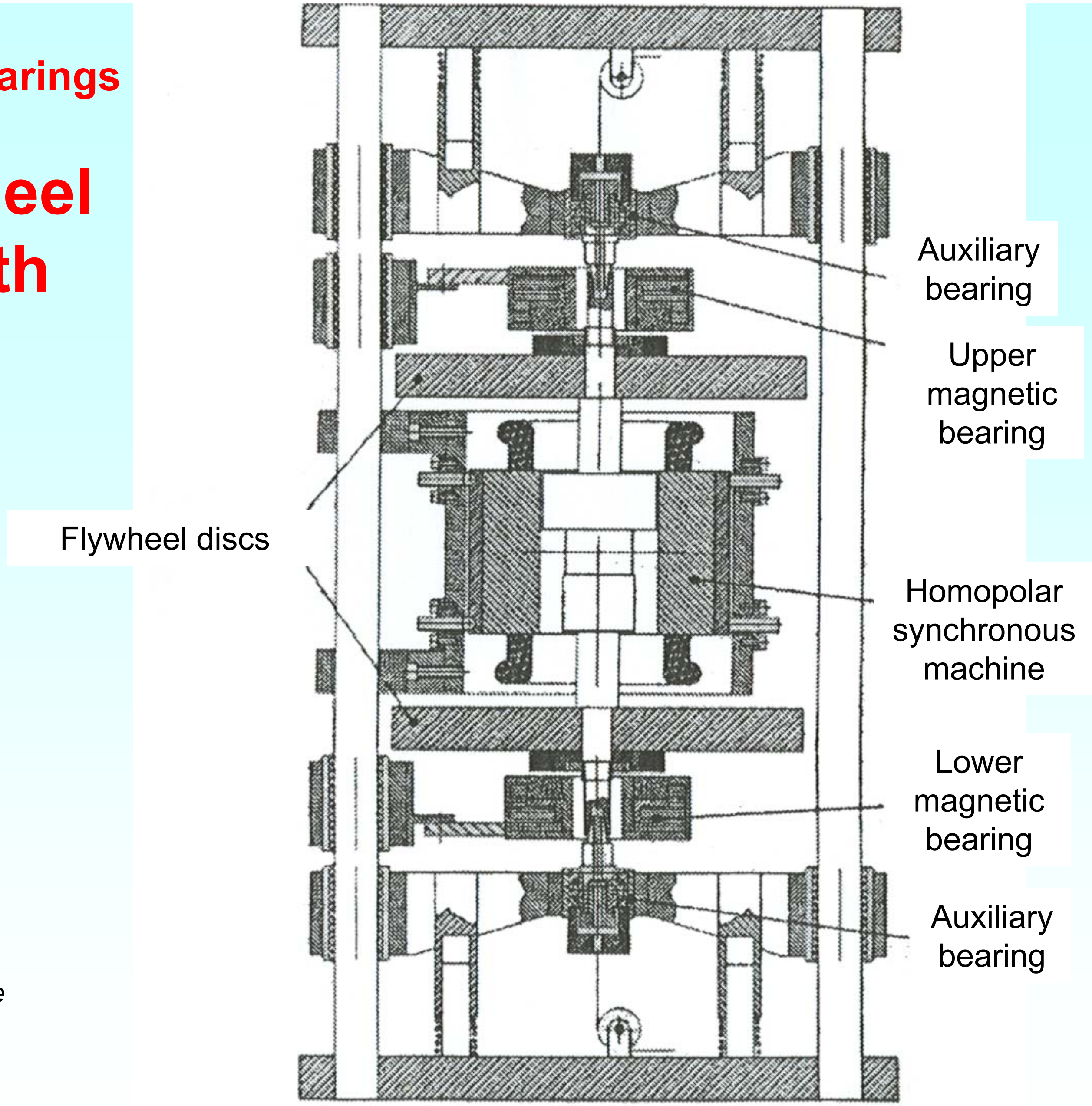

Source:

Uni. Stuttgart und FSZ Karlsruhe

Flywheel storage system with SC magnetic bearing

- - HTSC Y(123)-magnetic bearing
  - 4-pole homo-polar motor-generator

- - Stored energy 300 Wh at 50 000/min,
  - max. charge/discharge energy: 10 kW
  - Rotor mass (2 flywheels & homo-polar rotor): 10 kg
  - 2 HTSC bearings, LN_2-cooling, operated in vacuum at 0.21 Pa pressure
  - Measured bearing losses at 10000/min: 3.5 W,
  - Calculated at n_N = 50 000/min: 55 W bearing losses
  - Motor-/Generator efficiency: 97 %, converter efficiency: 97%

- Possible further development:

  Design of a bigger stationary system: 100 kWh / 1 MW, made of 2 modules (Total weight 10 tons),

  Per module:

  1 rotor with: 1 motor/generator, 4 flywheels, 8 HTSC bearing units

3.5 Superconducting magnetic bearings

Prototype flywheel storage system (Cut view)

- 30 Wh/kg
- 1000 W/kg

- Stored energy 300 Wh at 50000/min,
- max. charge-/discharge power: 10 kW
- P/m = 10 kW/10 kg = 1000 W/kg

Source:

Uni. Stuttgart und FSZ Karlsruhe

Different energy storage systems: *Ragone* diagram

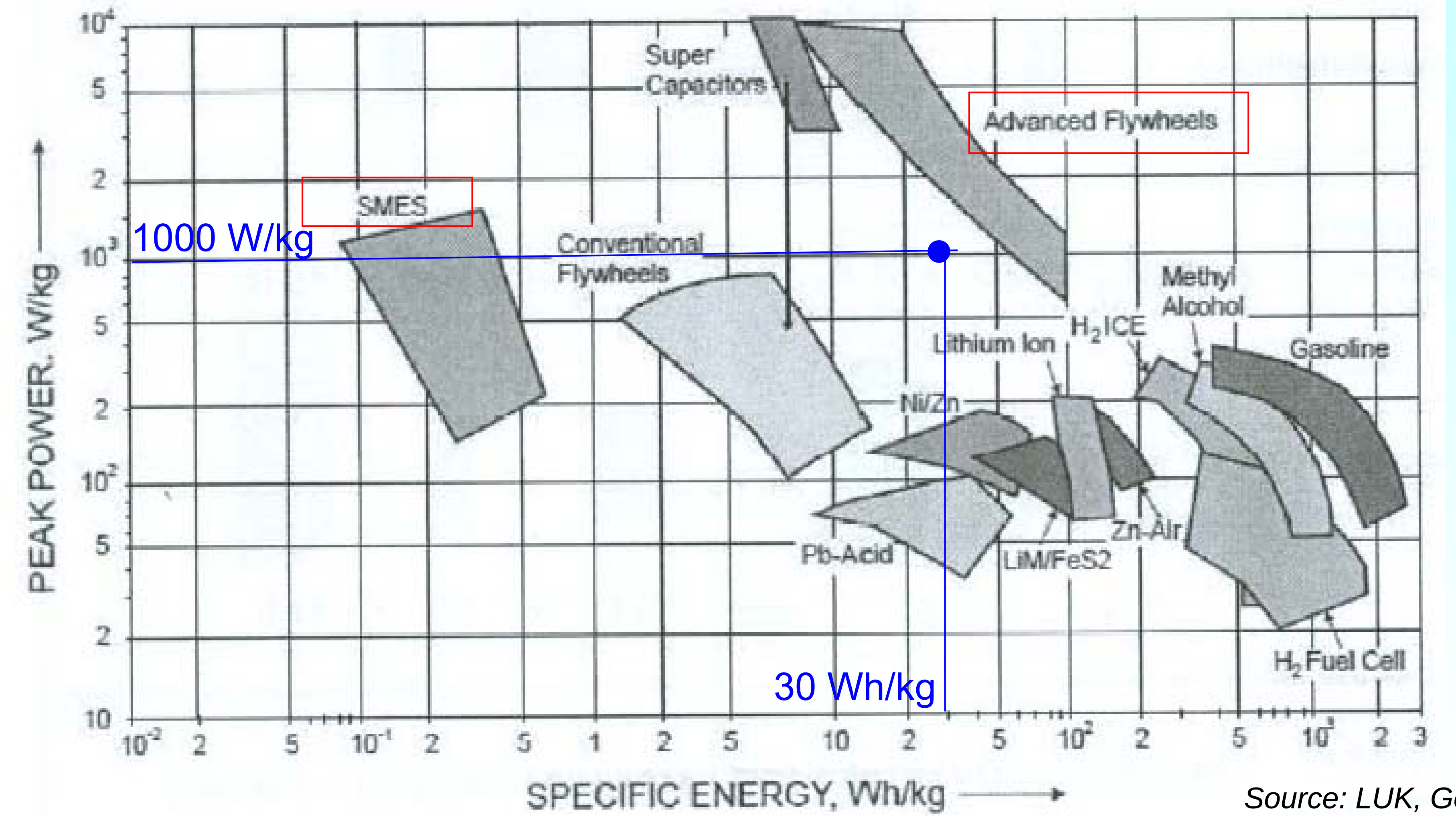

Source: LUK, Germany

Superconducting radial-axial high-gradient magnetic bearing

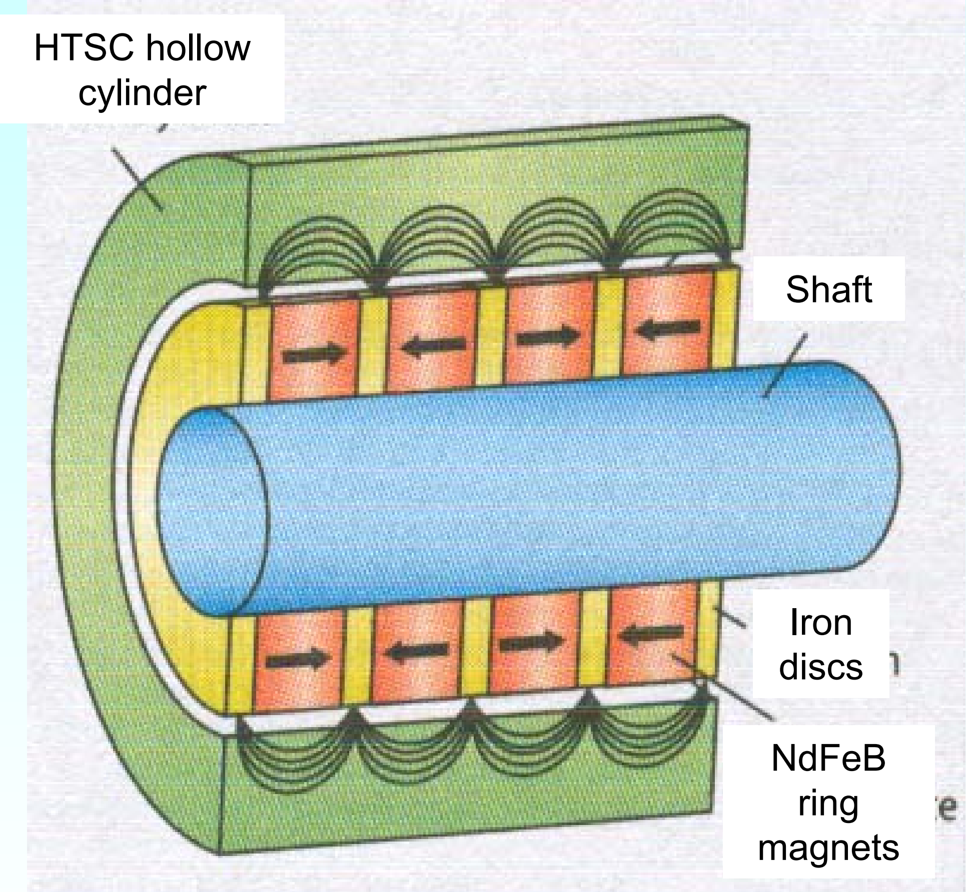

HTSC bearing: Layout

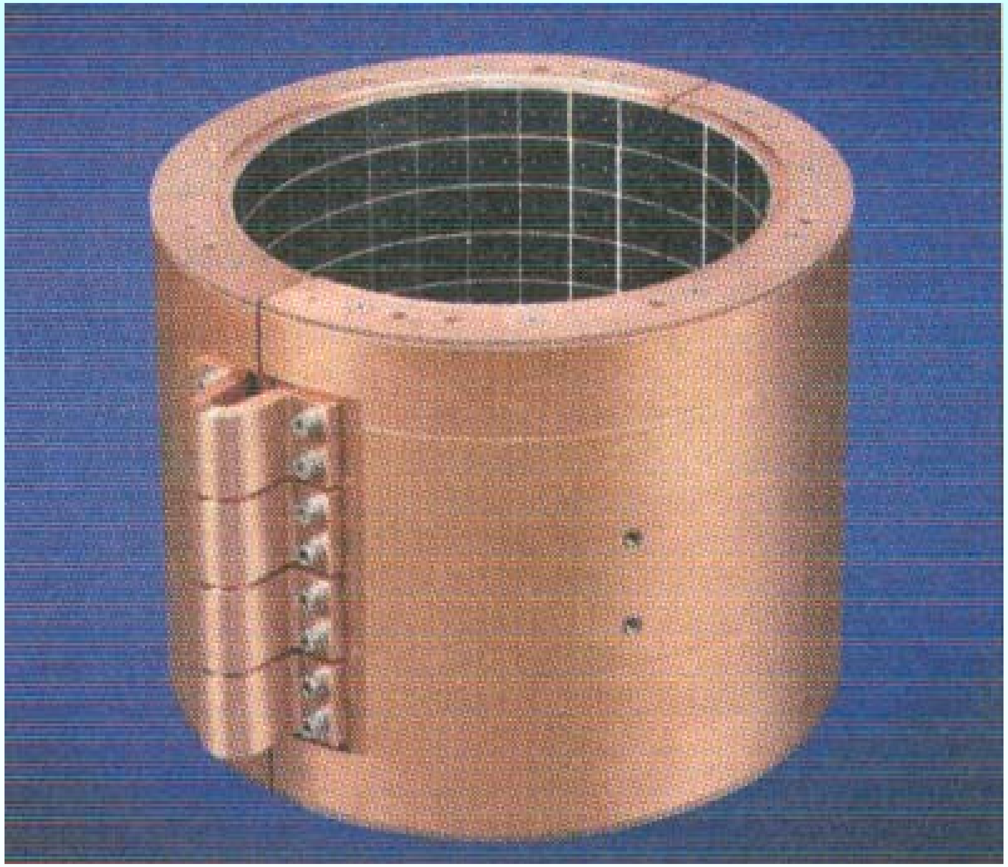

HTSC stator hollow cylinder

Source: Siemens AG, Erlangen, Germany

Superconducting radial-axial high-gradient magnetic bearing

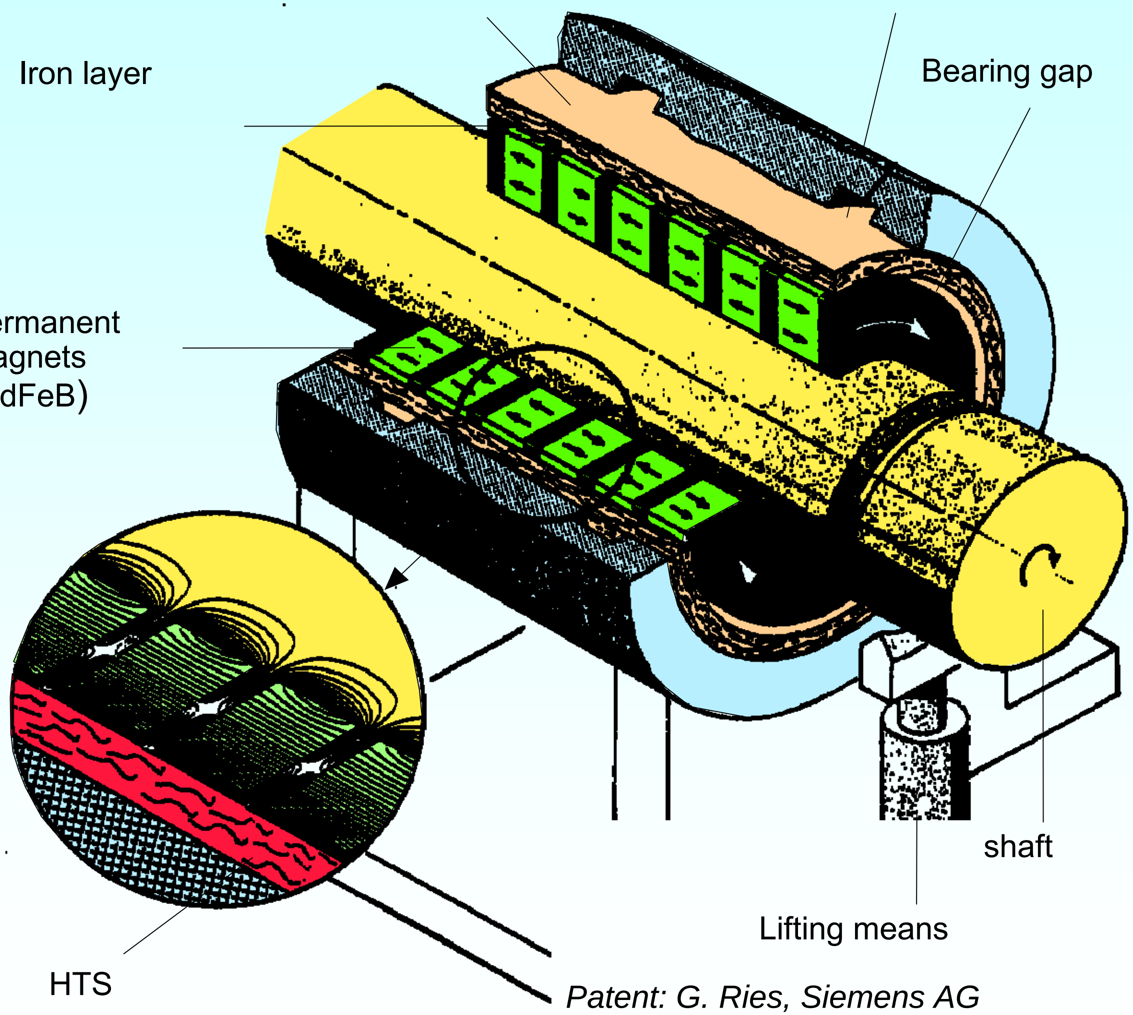

Patent: G. Ries, Siemens AG

Properties:

- No contact, no wear, no lubricant
- Self-stable behavior without external controlling
- Radial and axial levitation
- Low friction, high rotation speed
- Sufficient pre-warning time at loss of coolant

Applications:

- High speed machines
- Flywheel storage
- Oil free turbine bearings

Source: Siemens AG, Erlangen, Germany

High-gradient HTSC magnetic bearing for a 4-MVA-HTSC synchronous generator

- Radial static bearing force 5000 N
- Operation at 3600 /min
- Cold YBCO-stator in vacuum chamber
- LN_2-cooling with cooling head $T \leq 65$ K

Layout of first industrially used HTSC magnetic bearing (built by *Nexans*):

Diameter: ~ 65 cm
Length: ~ 40 cm
Height: ~ 150 cm
(Size is not optimized yet !)

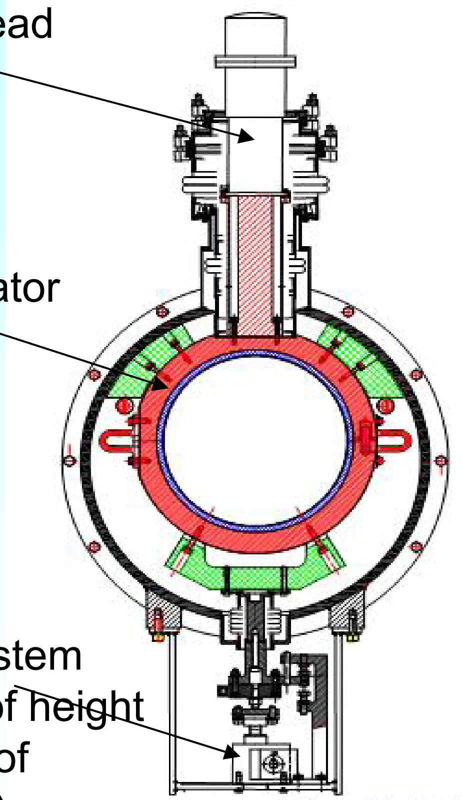

Source: Siemens AG, Germany

Passive HTSC magnetic bearing for 4-MVA-HTS-Generator

Radial bearing stiffness:
~ 5,1 kN/mm

Radial levitation force (with centered shaft):
~ 5 kN

Shaft oscillation at 3600 /min:
≤ ±5 µm

Rotation losses at 3600 /min:
~ 200 W

Source: Siemens AG, Germany

Estimate of equivalent friction coefficient for bearing losses

- Radial static bearing force F_n = 5000 N
- Total rotational bearing losses at n = 3600 /min: P_d = 200 W

$$P_d = F_t v_u = F_t d\pi n$$

$$F_t = P_d /(d\pi n) = 200/(0.32\cdot\pi\cdot 60) = 3.3\mathrm{N}$$

$$\mu = F_t / F_n = 3.3/5000 = 6.6\cdot 10^{-4}$$

Aim for low loss bearings in flywheel applications: $\mu = 10^{-6}$

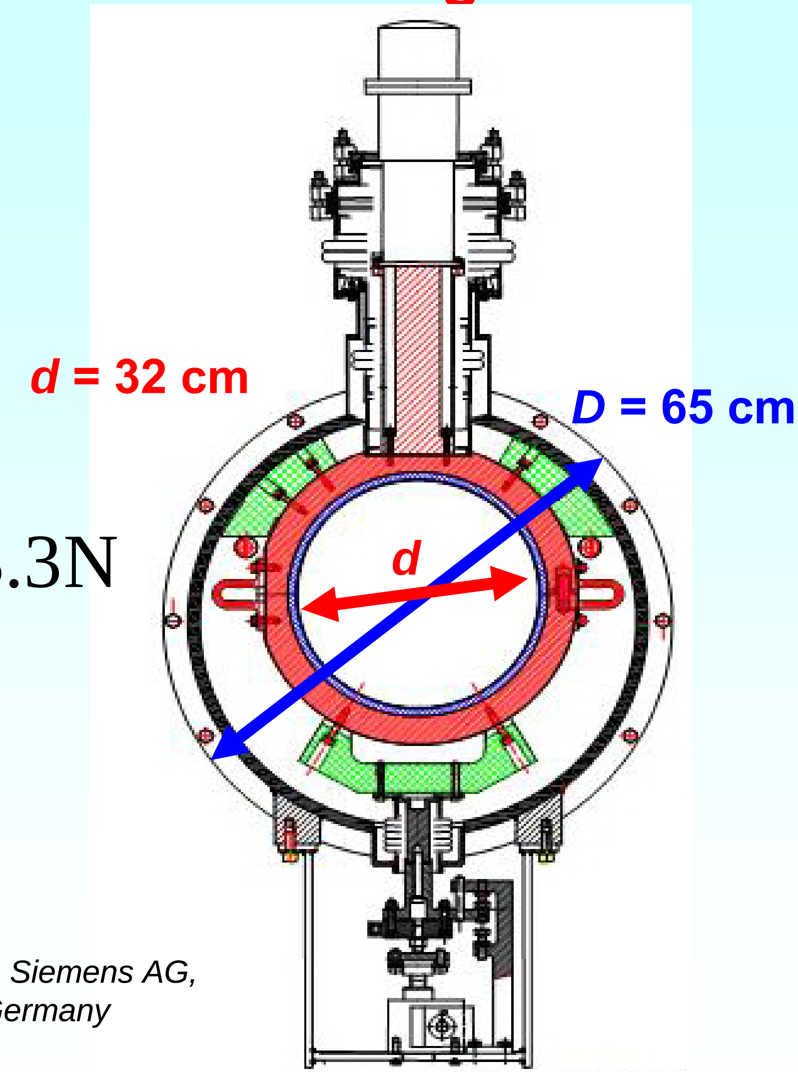

Source: Siemens AG, Germany

Summary:
Superconducting magnetic bearings

- Bulk Y-based superconductors „freeze“ the magnetic field
- Analog to *Meissner-Ochsenfeld* effect a self-stable levitation possible
- Limited size of SC bulk elements due to brittle material
- Higher bearing forces possible with larger bulk elements in the future
- Lowest losses of all known magnetic levitation systems
- Low temperature operation necessary
- Fly-wheel application